University of South-Eastern Norway

www.usn.no

FMH606 Master's Thesis 2024

Process Technology

Process simulation and cost optimization of amine based CO_2 capture integrated with a natural gas based power plant

Henrik Tahami

Faculty of Technology, Natural sciences and Maritime Sciences

Campus Porsgrunn

University of South-Eastern Norway

www.usn.no

Course: FMH606 Master's Thesis, 2024

Title: Process simulation and cost optimization of amine based CO_2 capture integrated with a natural gas based power plant

Number of pages: 82

Keywords: CO_2 capture, Gas-based power plant, Amine, Amine based CO_2 capture, , Aspen HYSYS, Dimensioning, Cost optimization

Student:	Henrik Tahami
Supervisor:	Lars Erik Øi, Solomon Aromada (co-supervisor)
External partner:	SINTEF Industry

University of South-Eastern Norway

www.usn.no

Summary:

Combining gas-fired power plants equipped with CO2 capture systems is an efficient and cost-effective method for reducing carbon dioxide emissions from flue gases, thereby mitigating greenhouse gas emissions and combating global warming and climate change. The use of amine-based solvents for CO_2 removal from exhaust gas is a well-established and effective process.

In this study, a base case scenario was modeled in Aspen HYSYS employing input data from previous studies on the integration of CO_2 capture plant and NGCC (Natural Gas Combined Cycle). The base case simulation design included setting key parameters such as turbine inlet temperature (1500 °C), power generation of the combined cycle (400 MW),75 °C as the minimum temperature approach in the evaporator (ΔT_{min}), CO_2 removal efficiency (90%), minimum temperature approach in the lean/rich heat exchanger (10 °C), and flue gas inlet temperature to the absorber (40 °C). The Enhanced Detailed Factor (EDF) and net present value (NPV) techniques as well as Aspen In-Plant Cost Estimator software, were employed to guess the total cost of the base case model, considering CAPEX, OPEX, and income from power sales. The cost evaluation revealed a net present value of €289 million over project lifetime (a 25-year), with a 16-year payback period following project implementation. Sensitivity analysis was conducted to optimize costs, using the power law method to estimate equipment costs when their sizes were changed. Parameters such as ΔT_{min} in lean/rich heat exchanger, and the evaporator's minimum temperature approach were adjusted to maximize the project's NPV. The other parameter was the exhaust gas recirculation (EGR) ratio. EGR is the portion of the heat recovery steam generators exhaust gas, which is recirculated back to the gas turbine inlet

The cost-optimized parameters identified from the sensitivity analysis included a zero EGR ratio, ΔT_{min} of 20 °C in lean/rich heat exchangers, and ΔT_{min} of 65 °C in evaporators. Also a python code was written to perform this automatic sensitivity calculation by calling HYSYS from Python.

The primary objective of this study was to use the Aspen HYSYS software to calculate cost and estimate cost optimum process parameters of a gas-based power plant which is integrated with an MEA-based CO_2 capture system. This work is innovative in its inclusion of a sensitivity analysis on the EGR ratio and the evaporator's minimum temperature approach with this integrated model, which has not been previously addressed in similar studies.

Preface

This report has been prepared for a master's thesis entitled “Process Simulation and Cost Optimization of Amine-Based CO_2 Capture Integrated with a Natural Gas-Based Power Plant” at the University of South-Eastern Norway (USN). The primary goal of this thesis is to simulate and estimate the costs of the amine-based CO_2 capture plant using Aspen HYSYS and Aspen In-Plant Cost Estimator, respectively as well as cost optimization of operating parameters.

I would like to express my gratitude to the supervisor of this thesis, Professor Lars Erik Øi of USN. Completing this thesis would have been impossible without his kind assistance and valuable comments. He not only provided helpful feedback but also held regular weekly meetings throughout the semester to discuss the project and guide me in the right direction.

Alo received assistance from Solomon Aforkoghene Aromada, who was instrumental in completing this project. He facilitated my use of the Aspen In-Plant Cost Estimator for conducting the cost estimation analysis.

I would also like to extend my heartfelt thanks to Esmaeel Aboukazempour Amiri, who assisted me with modeling and simulation and contributed valuable ideas to the project.

Porsgrunn, 2024

Henrik Tahami

Contents

Nomenclature

Abbreviation	Explanation
CCUS	CO_2 capture, utilization and storage
AC	Absorption capacity
MEA	Monoethanolamine
EDF	Enhanced detailed factor
CAPEX	Capital expenditure
OPEX	Operational costs
EIC	Equipment installation cost
MEUR	Million euro
PFD	Process flow diagram
STHE	Shell and tube heat exchanger
PHE	Plate heat exchanger
CHP	Combined heat and power plant
NGCC	Natural gas combined cycle
EGR	Exhaust gas recirculation
HTU	Height of transfer unit
LMTD	Logarithmic mean temperature differential
IGCC	Integrated gasification combined cycle
ASU	Air separation unit
CPU	Compression and purification unit
FB	Fluidized bed
CLC	Chemical looping cycle
LHV	Low heating value
NPV	Net present value
PBP	Payback period
HEX	Heat exchanger
CCGT	Combined cycle gas turbine
CCPP	Combined cycle power plant

1 Introduction

Over the next few decades, global electricity consumption is expected to rise significantly due to structural changes, economic growth, and increased electrification [1]. The Energy Institute's Statistical Review of World Energy presents data on the use of various energy sources worldwide from 1965 to 2022 [2]. Figure 1.1 illustrates this data for 2022, showing that fossil fuels, including oil, coal, and gas, are the primary sources of energy to meet current demand. However, limited resources and environmental pollution have become major issues associated with fossil fuels [3]. If not properly managed, these primary fuel sources will greatly impact the planet's climate and weather patterns.

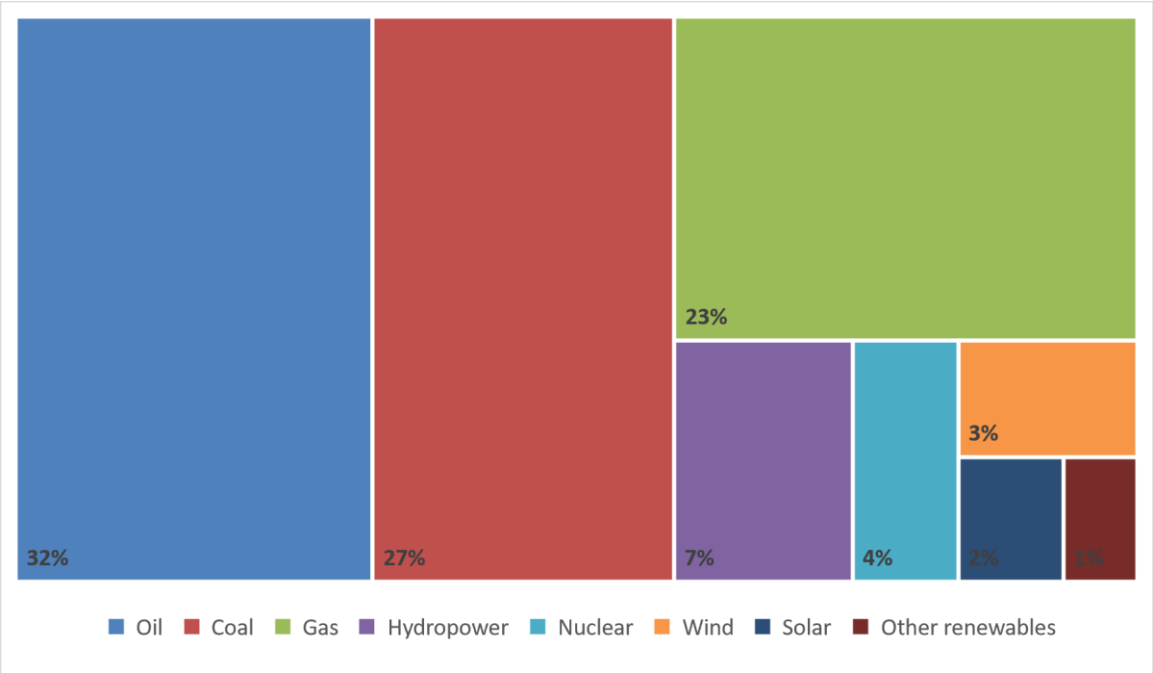

Figure 1.1: Share of energy consumption in the world between different sources in 2022 [2].

Capitalist democracy depends on hydrocarbons, and fossil fuels are not expected to be depleted soon [4]. From 2013 to 2019, oil reserves increased by 27%, matching the growth seen from 2003 to 2013 [4]. Additionally, historical data shows that while new energy sources have been successfully integrated into the global energy system and now make up a significant portion of the total energy supply, it is rare for these additions to lead to a long-term decrease in fossil fuel use [5]. Therefore, it is essential to find environmentally friendly ways to utilize these resources.

1.1 Background

According to the IEA report, fossil fuels are the primary source of CO_2 emissions globally. Despite this, they remain a crucial part of the world's energy resources, and their significance may even grow in the future [6].

To mitigate the effect of carbon dioxide discharges from fossil fuel power plants, carbon capture and storage is among the most effective solutions, along with enhancing power plant efficiency and adopting green energy technologies [7].

Among fossil fuels, natural gas stands out as one of the most practical and efficient energy sources. Utilizing natural gas in combined cycle power plants is a modern technology that offers the greatest efficiency compared to other fossil fuels. For instance, coal power plants release double as much carbon dioxide as natural gas power plants [8].

Despite natural gas power plants producing and emitting less carbon dioxide than other fossil fuel power plants, they remain a significant source of carbon dioxide emissions [7].

There are three major CO_2 capture methods used in combustion operations: pre-combustion capture, oxygen combustion as well as post-combustion capture, as illustrated in Figure 1.2. Of these methods, post-combustion capture is the most common and effective for fossil fuel power plants and further industries [9].

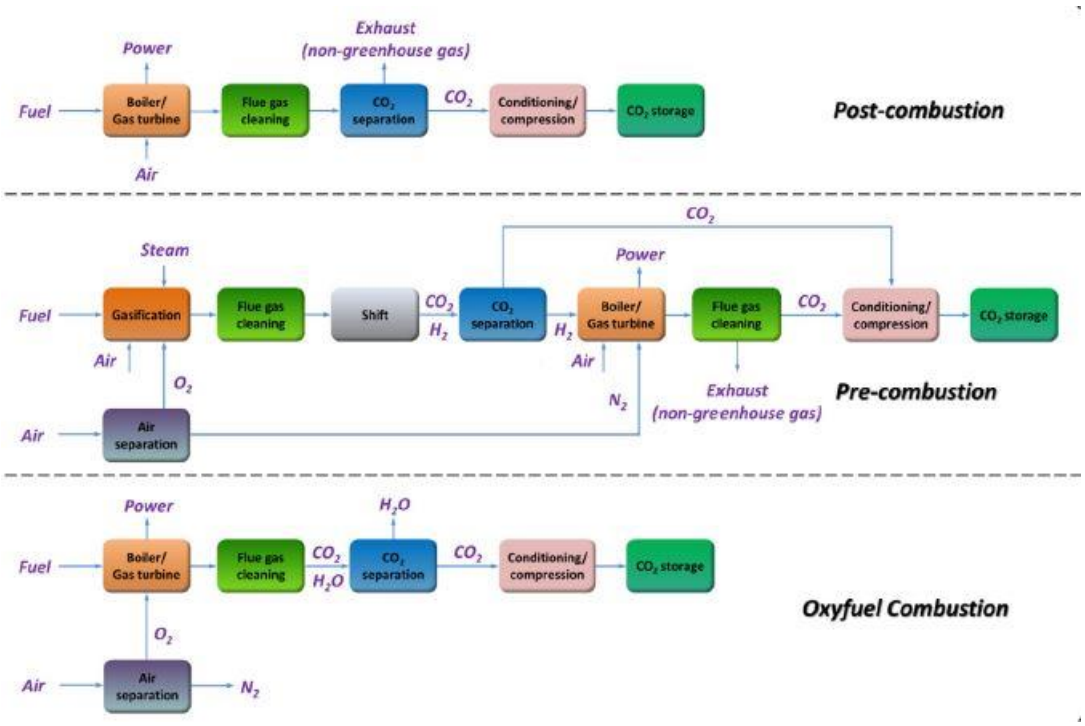

Figure 1.2: The prevalent methods of reducing CO_2 emissions from using fossil fuels [10].

A key point regarding post-combustion CO_2 capture is that it accounts for upwards of 70% of the total price of the carbon capture and storage process, making it the most costly component [11]

Common methods for post-combustion CO_2 capture include chemical absorption using aqueous amine solutions [12], adsorption [13], cryogenic separation [12], membrane separation [12], and microalgal systems, as detailed in Figure 1.3

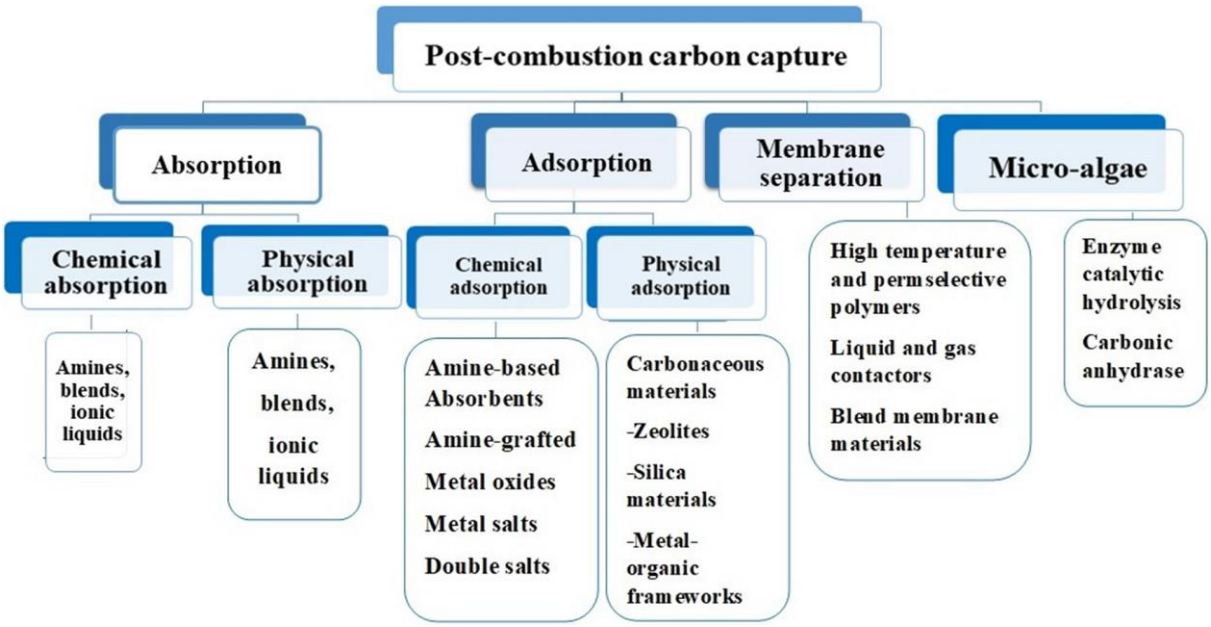

Figure 1.3: Post-combustion CO_2 capture technologies [14]

Of the methods mentioned, the chemical absorption/stripping process using MEA for desorption is the most suitable and practical technology. It can be effectively integrated with NGCC power plants to ensure efficient operation [15]

1.2 Literature review

The aim of this part is to review and analyze the key literature on the design, simulation as well as dimensioning and cost optimization of a combined natural gas combined power plant equipped with CO_2 capture units. While numerous studies have focused on standalone CO_2 capture plants, there is a scarcity of research on integrated capture and power plants. The most significant literature in this area is summarized in Table 1.1, organized by the year of publication.

Table 1.1: A literature overview

No.	Reference	Year	Title of the literature
1	[15]	2007	Aspen HYSYS Simulation of CO_2 Removal by Amine Absorption from a Gas Based Power Plant
2	[16]	2011	Combining bioenergy and CO_2 capture from gas fired power plant
3	[17]	2011	Impacts of exhaust gas recirculation (EGR) on the natural gas combined cycle integrated with chemical absorption CO_2 capture technology
4	[18]	2012	Removal of CO_2 from exhaust gas
5	[19]	2012	Natural Gas Combined Cycle Power Plant Integrated to Capture Plant.
6	[20]	2012	Natural gas combined cycle power plants with CO_2 capture – Opportunities to reduce cost
7	[21]	2015	Heat integration of natural gas combined cycle power plant integrated with post-combustion CO_2 capture and compression
8	[22]	2016	Optimal operation of MEA-based post combustion carbon capture for natural gas combined cycle power plants under different market conditions
9	[23]	2016	Techno-economic process design of a commercial-scale amine-based CO_2 capture system for natural gas combined cycle power plant with exhaust gas recirculation.
10	[24]	2016	A techno-economic analysis of post-combustion CO_2 capture and compression applied to a combined cycle gas turbine: Part I. A parametric study of the key technical performance indicators.
11	[25]	2016	A techno-economic analysis of post-combustion CO_2 capture and compression applied to a combined cycle gas turbine: Part II. Identifying the cost-optimal control and design variables

12	[26]	2017	Thermodynamic analysis and techno-economic evaluation of an integrated natural gas combined cycle (NGCC) power plant with post-combustion CO_2 capture.
13	[27]	2017	Selection and design of post-combustion CO_2 capture process for 600 MW natural gas fueled thermal power plant based on operability.
14	[28]	2018	A new integration system for natural gas combined cycle power plants with CO_2 capture and heat supply.
15	[29]	2019	Optimization of Post Combustion CO_2 Capture from a Combined-Cycle Gas Turbine Power Plant via Taguchi Design of Experiment
16	[30]	2020	Preliminary performance and cost evaluation of four alternative technologies for post-combustion CO_2 capture in natural gas-fired power plants.
17	[31]	2021	A simulation study of the effect of post combustion amine-based carbon-capturing integrated with solar thermal collectors for combined cycle gas power plant.
18	[32]	2023	Process simulation and cost optimization of gas-based power plant integrated with amine-based CO_2 capture

Lars Erik Øi [15] simulated simplified merged cycle gas power plant and an MEA (monoethanolamine) based CO_2 removal process utilizing Aspen HYSYS. In this work thermodynamic properties were computed using the Peng Robinson and Amines Property Package models offered in Aspen HYSYS. Adiabatic efficiencies in gas turbines, and steam turbines and compressors were adjusted to attain 58% as the total thermal efficiency in the natural gas power plant with no CO_2 removal. This efficiency drops to approximately 50% with CO_2 removal. The percentage of CO_2 removal and energy intake in the CO_2 removal plant were calculated based on the amine circulation rate, absorption temperature, absorption column height as well as steam temperature. For 85% CO_2 removal, the heat consumption was calculated to be 3.7 MJ/kg of CO_2 removed, which is close to the literature value of 4.0 MJ/kg CO_2 [15].

Lars Erik Øi's Ph.D. thesis [16] concentrated on optimizing CO_2 removal from the exhaust gases of a natural gas combined cycle power plant. The research aimed to identify the most cost-effective parameter values. Øi examined both the split stream process, which consumes

3 GJ of heat per ton of CO_2 removed, and the standard process, which consumes 4 GJ per ton. The optimal calculations revealed that the gas inlet temperature should be maintained between 33 and 35°C, the minimum temperature difference in the lean/rich amine heat exchanger should range from 12 to 19°C, and the rich amine loading should be 0.47 mol CO_2 per mol MEA. Additionally, he assessed the best automation strategies for these parameters [16].

Le et al. [17] demonstrated that increasing the CO_2 concentration in the exhaust gas is a hypothetically effective method for reducing the significant electrical efficiency penalty associated with chemical absorption. Adjusting the exhaust gas recirculation (EGR) ratio alters the exhaust gas mass flow as well as CO_2 concentration delivered to the chemical absorption unit. In their research, the effects of EGR on a combined gas turbine cycle were quantitatively analyzed concerning the energy requirements of MEA-based chemical absorption. Their simulations indicate that, compared to a combined cycle without EGR, a recirculation ratio of 50% can raise the CO_2 concentration from 3.8 mol% to 7.9 mol% and decrease the mass flow of the absorber feed stream by 51.0%. Consequently, the total thermal energy consumption of the reboiler is reduced by 8.1%. From an electrical efficiency perspective, the optimal EGR ratio is around 50%, which can enhance the overall efficiency by 0.4 percentage points of NG LHV compared to a system without EGR. Additionally, EGR lowers the O2 concentration in the exhaust gas. While low oxygen concentration may negatively impact combustion stability and completeness, these effects can be mitigated through oxygen enrichment or novel combustor designs. On the positive side, it may lead to reductions in NOX emissions and amine degradation [17].

Eldrup et al. [18] explored a system combining natural gas power generation with CO_2 capture, using biomass-based external energy plants. They compared this concept to other alternatives by estimating both capital and operational costs. The operating cost estimates took into account the need to buy CO_2 credits for each ton of non-bio-based CO_2 emitted and to earn CO_2 credits for each ton of bio-based CO_2 captured. This approach proves to be economically viable when biomass prices are low and CO_2 credit prices are high. Through a sensitivity analysis, they examined varying prices for natural gas, CO_2 credits, and biomass. The proposed strategy shows the most benefit when CO_2 credit prices increase [18].

Karimi et al. [19] evaluated a natural gas combined cycle (NGCC) power plant with a power of approximately 430 MW, paired with a solvent absorber/stripper CO_2 capture plant. The system achieves a 90% CO_2 removal rate, with the captured CO2 being compressed to 75 bars, liquefied, and then pumped to 110 bars. The CO_2 capture process incurs an energy penalty of 398.4 kWhel/ton, reducing the plant's net efficiency by 7.5%. This energy penalty is attributed to steam extraction as well as electricity consumption, which account for 4.6% and 2.9% of the penalty, respectively [19].

Sipöcza and Tobiesen [20] conducted a thermodynamic and economic analysis of a 440 MWe CO_2 removal plant combined with a natural gas combined cycle power plant, using an aqueous monoethanolamine (MEA) solution. Their flow sheet for the CO_2 capture plant included

absorber inter-cooling and lean vapor recompression, optimized for process parameters. The gas turbine utilized a 40% exhaust gas recirculation (EGR) rate to further reduce CO_2 capture costs, effectively doubling the CO_2 concentration in the exhaust gas compared to conventional gas turbines. This combination of reduced specific reboiler duty and EGR significantly lowered both capital and operating costs. Moreover, the study highlighted that precise cost estimates are heavily affected by fluctuations in fuel prices and currency exchange rates [20].

Luo et al. [21] conducted a study on integrating a 453 MW NGCC power plant among a CO_2 compression train coupled with MEA-based post-combustion carbon capture (PCC) technology. They used Aspen Plus to create and validate steady-state models for the NGCC power plant, PCC process as well as compression train, utilizing both documented and experimental data. Their analysis revealed that using exhaust gas recirculation (EGR) significantly reduced the size of the absorber and stripper. The integration of the NGCC power plant with the PCC process and compression led to a decrease in net efficiency from 58.74% to 49.76% (based on low heating value, LHV). However, implementing EGR increased the overall efficiency to 49.93%, and incorporating two different methods for integrating compression heat further boosted efficiency to 50.25% and 50.47%, respectively [21].

Luo and Wang [22] conducted a study to evaluate the operation of a NGCC power plant integrated with a post-combustion carbon capture system under various market conditions. They focused on cost optimization, using the levelized cost of electricity (LCOE) as the objective function. An economic evaluation was performed for the integrated system's baseline scenario, which included CO_2 transport and storage. The analysis revealed that the carbon price needs to exceed €100/ton CO_2 to justify the cost of carbon capture from the NGCC power plant, and it must surpass €120/ton CO_2 to achieve a 90% carbon capture rate [22].

Recirculating exhaust gas is a method to increase CO_2 concentration in the flue gas for natural gas power generation systems. Ali et al. [23] studied this technique and developed four specific amine-based CO_2 capture devices, achieving a 90% capture rate with a 30% aqueous amine solution. They documented design outcomes for a 650 MWe natural gas-fired combined cycle power plant, considering EGR percentages of 20%, 35%, and 50%. For a gas-fired power plant without EGR, the ideal liquid-to-gas ratio for the amine-based CO_2 capture plant is 0.96. When EGR is applied, the liquid-to-gas ratios are 1.22 at 20%, 1.46 at 35%, and 1.90 at 50%. These results suggest that using EGR in natural gas-fired power plants can reduce the energy demand and financial costs of amine-based CO_2 capture facilities [23].

Alhajaja et al. [24] designed and evaluated a CO_2 capture plant and compression train model using monoethanolamine (MEA). After validating the model, they evaluated key operating parameters based on selected non-monetized economic as well as environmental performance indicators to determine their impact on the CO_2 capture as well as compression process for a CCGT. The results indicated increased compression power requirements and a significant rise in cooling water demand for coolers and washing water systems. This study highlights the

challenging trade-offs between minimizing environmental impacts and managing capital and operational expenditures [24].

Alhajaj et al. [25] observed in the second part of their study that utilizing the bypass option for CO_2 capture is the most cost-effective solution when the total degree of capture (DOC) is below 60%. They found that carbon prices significantly influence the cost-optimal DOC, shifting it from 70%-80% to 85%-90% as carbon prices increase from \$4/t CO_2 to \$23/t CO_2 [25].

Xu et al. [26] proposed an innovative system combining electricity generation and CO_2 capture to reduce the decarbonization penalty. The system employs four strategies: recycling flue gases from the gas turbine to increase CO_2 levels in the combustion gases, using condensate water from the boiler with exported steam to utilize the extracted steam's superheat, compressing CO_2 at the stripper's upper side to recover latent heat for sorbent recovery, and introducing a trans critical CO_2 cycle to harness sensible heat in the exhaust gas. This integration results in a power production increase of 26.15 MW compared to a standard NGCC plant without decarbonization. The CO_2 capture efficiency penalty is reduced by 2.63 percentage points, while the investment increase of \$60.17 million represents only a 4.66% rise compared to a non-integrated decarbonization plant [26].

Dutta et al. [27] examined the design and operation of a post-combustion CO_2 capture (PCC) facility for a natural gas power plant. They evaluated two enhanced PCC system designs, each with minimal efficiency penalties. Design considerations included operability and absorber construction constraints, which influenced equipment sizing. They studied two absorber designs based on full flue gas flow and the average load fluctuation of a flexible power plant. Designing for time-average load reduced absorber purchase costs by 4%, and the absorber's reboiler duty was optimized to maintain capture rates under part-load conditions [27].

Hu et al. [28] proposed an integrated model combining power generation, CO_2 capture, and heat supply, employing techniques to recycle waste heat from the CO_2 capture process: steam recirculation, a CO_2 Rankine cycle as well as radiant floor heating. The radiant floor heating subsystem efficiently recycles low-temperature waste energy from the absorbent cooler. Thermodynamic analysis showed the new system produces 19.48 MW more power than a decarbonizing NGCC plant without heat integration, with the radiant floor system reclaiming 247.59 MW of heat, boosting total energy efficiency to 73.6%. This integration requires only 2.6% more capital investment and generates an additional \$3.40/MWh, reducing CO_2 capture costs by 22.3% [28].

Soltani et al. [29] simulated 90% CO_2 capture for a 600 MW NGCC power plant using an equilibrium-based method in Aspen Plus. They analyzed the effects of inlet exhaust gas temperature, absorber column pressure, exhaust gas recirculation volume, and amine concentration. Optimal values—50°C exhaust gas temperature, 1 bar absorber pressure, 20% flue gas recirculation, and 35 wt.% amine concentration—minimized specific energy

requirements, with amine concentration having the highest priority. The total energy required for CO_2 capture was 5.05 GJ/ton, and the boiler required 3.94 GJ/ton [29].

Gatti [30] evaluated four post-combustion CO_2 capture techniques for natural gas-fired power plants: CO2 permeable membranes and molten carbonate fuel cells and pressurized CO_2 absorption with a multi-shaft gas turbine and heat recovery steam cycle, as well as supersonic flow CO_2 anti-sublimation and inertial separation. Using an NGCC without CO_2 capture as a reference, and an NGCC with MEA-based capture as the base case, the study found MCFCs to be the most promising in terms of economics and energy penalty, with a CO_2 avoided cost of \$49/t CO_2 and a SPECCA of 0.31 MJLHV/kg CO_2. PZ scrubbing was the next best (SPECCA = 2.73 MJLHV/kg CO_2, CO_2 cost saved = \$68/t CO_2), followed by MEA (SPECCA = 3.34 MJLHV/kg CO_2, CO_2 cost saved = \$75/t CO_2), and then supersonic flow and CO_2 membranes [30].

Ayyad et al. [31] conducted an economic analysis of the 495 MW West Damietta power plant in Egypt to reduce reboiler duty and associated power loss. They explored recycling flue gas back into the combustor at ratios up to 35% and using parabolic-trough solar collectors to offset the boiler load instead of low-pressure steam. Results showed a significant reduction in reboiler duty up to 20% with increased carbon content. The levelized cost of energy (LCOE) decreased by 1.39%, and the cost of avoiding carbon emissions dropped by 6% at a 35% recirculation ratio. Integrating a solar system and thermal energy storage significantly enhanced the plant's production capacity [31].

In Aboukazempour Amiri’s thesis [32], he integrated a gas-based power plants with CO_2 capture plant in a simulation model .His base case setup was modeled in Aspen HYSYS using input data from other research on natural gas-fired power plants. In this work, key parameters were set as follows: turbine inlet temperature at 1500 °C, power generation at 400 MW, CO_2 removal efficiency at 85%, lean/rich heat exchanger approach temperature at 10 °C, and absorber inlet temperature at 40 °C. The overall cost of the base case model was estimated using the Aspen In-Plant Cost Estimator tool, Enhanced Detailed Factor method, and net present value (NPV) method, considering CAPEX, OPEX, and revenue from power sales. The results showed an NPV of €1570 million over a 25-year plant lifetime and a seven year payback period. Also, sensitivity analysis was conducted for cost optimization, altering parameters such as ambient temperature, inlet air/gas pressure, flue gas outlet temperature, lean/rich heat exchanger approach temperature, number of absorber stages, and flue gas inlet temperature to maximize NPV. Optimal conditions were found to be an ambient temperature of 10 °C, inlet air/gas pressure of 25 bar, off-gas temperature of 50 °C, lean/rich heat exchanger approach temperature of 13 °C, 10 absorber stages, and inlet flue gas temperature of 30-35 °C. The sensitivity analysis results were used to update the base case, resulting in an average 15% raise in profit compared to the primary scenario [32].

1.3 Scope of the study

This research primarily focuses on the integration and cost optimization of a natural gas combined cycle (NGCC) plant with an amine absorption CO_2 capture system. The simulation is conducted using Aspen HYSYS version 12, based on data from a previous study by Aboukazempour Amiri [32]. Initially, separate simulations for the natural gas power plant and the CO_2 capture plant were designed in Aspen HYSYS. These simulations were then combined into a single flow sheet, followed by dimensioning and cost estimation based on the new flow sheet. The Aspen In-Plant Cost Estimator, utilizing the Enhanced Detailed Factor, was used to estimate and assess the total cost for the basic setting. Cost optimization was performed using sensitivity analysis to identify and reduce costs. To understand the impact of operational parameters on the total cost, a sensitivity analysis was carried out. The Power-Law approach was employed to update equipment costs, and the NPV value was used for cost optimization evaluation. As part of this investigation, the exhaust gas recirculation (EGR) ratio, the evaporator's minimum temperature approach, and the lean/rich amine heat exchanger's minimum temperature approach were all subjected to sensitivity analysis. The goal was to calculate the optimal values of these operating parameters to achieve 90% CO_2 removal while generating 400 MW of electricity and maintaining a combustion chamber temperature of 1500 °C.

Appendix A displays the task description of this thesis.

2 Process description

This chapter offers an overview and process description of natural gas combined cycle power plants and CO_2 capture plants.

2.1 Natural gas combined power plant

Combined-cycle power plants generate electricity by using the exhaust heat from a gas turbine to power a steam turbine and operate a boiler , which then produces steam to drive a steam turbine. These plants produce 50% more electricity than simple-cycle plants and achieve efficiencies of 50%–60% while maintaining low emissions [33].

The gas turbine operates on the Brayton cycle, powered by the combustion byproducts of the fuel, while the steam turbine operates on the Rankine cycle, driven by steam generated by the Heat Recovery Steam Generator (HRSG) from the latent heat of the gas turbine's exhaust gases [31]. The primary components of a combined cycle power plant include:

- Gas turbine
- Steam turbine
- Heat recovery steam generators
- Condensers

The major parts and the diagram of the natural gas combined power plant are shown in Figure 2.1.

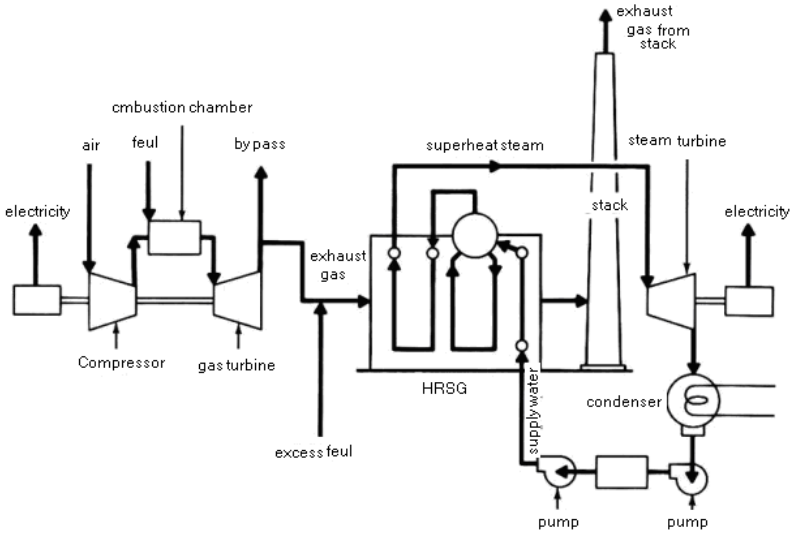

Figure 2.1: Representation of combined-cycle power generation [34]

2.1.1 Gas Turbine

In combined cycle power plants, gas turbines convert natural gas or fluid into mechanical energy. These turbines consist of three main components: the compressor, combustor, and generator. The compressor pressurizes the air, which then mixes with fuel in the combustor where it burns at constant pressure. The resulting hot gas flows through the turbine to generate work [35].

These turbines operate on the Brayton cycle, which ideally includes two isobaric processes and two isentropic processes. The gas turbine combustor system as well as the heat rejection side, and the heat recovery steam generators sides are isobaric processes. In the gas turbine, the compressor and the turbine expander correspond to the two isentropic processes [35].

The power balance in turbines consists of the outputs from both the gas and steam turbines, as well as the energy required to operate auxiliary equipment like pumps and compressors.

2.1.2 Steam Turbine

Steam turbines convert the energy in steam into mechanical work that drives the turbine's shaft (in the CCPP). The energy obtained by the steam turbine depends on the enthalpy drop, which is determined by the steam's temperature and pressure. The enthalpy of steam varies with these parameters, and the available energy can be calculated using a Mollier diagram if the input and output temperatures and pressures are known [36].

Steam turbines operate in three control modes [35]:

- Fixed Pressure Mode: When the load is below 50%, corresponding to about 50% of the live steam pressure, the steam turbine operates in fixed pressure mode. The main control maintains a constant steam generator pressure in this mode. If the steam turbine does not use all the output steam, the steam generator's bypass valves regulate the pressure.
- Sliding Pressure Mode: Once the load exceeds 50%, the primary control valve fully opens, and the steam turbine switches to sliding pressure mode. Here, the live steam pressure varies directly with the steam flow as the gas turbine load increases.
- Load Control: After synchronization with the grid, the generator's frequency is controlled by the grid. The turbine controller adjusts the steam flow to maintain the baseload.

2.1.3 Heat recovery steam generators

Recently, heat recovery steam generators (HRSGs) have gained popularity. They are often paired with gas turbines, using the steam to generate additional electricity. Combined-cycle units are very efficient in electricity generation and can operate at partial loads [36].

The HRSG receives exhaust gases from the gas turbine. These gases are cooled by steam/water coils in a counterflow direction, transferring heat to the steam/water. The temperature of the flue gas at the stack is approximately 110°C, but for very clean and sulfur-free fuel gases, it can be as low as 93°C [35].

Functioning similarly to a heat exchanger, the HRSG transports steam or water through tubes while flue gas flows on the shell side. It also includes steam drums that separate the generated steam from the boiling water before it is fed into the superheaters, thereby functioning similarly to a boiler [35].

The HRSG can have one, two, or three pressure levels depending on the plant size. For plants with a capacity of 200–400 MW, high-pressure (HP), intermediate-pressure (IP), and low-pressure (LP) levels are used. Plants under 60 MW typically have two pressure levels (HP and LP), while smaller plants have just one. In some cases, the LP section is used solely to provide steam for deaeration when three pressure levels are present [36].

2.1.4 Condensers

Condensing steam turbines are the most prevalent type of large steam turbines. They can be either air-cooled or water-cooled, with water-cooled condensers being more common and more efficient. The performance of the low-pressure (LP) steam turbine heavily depends on the condenser's cooling capacity. Reduced cooling efficiency increases the back pressure in the LP steam turbine, thereby decreasing its power output [35].

2.2 Amine based CO_2 capture process description

The most widely used and extensively studied technique for CO_2 removal involves using an amine solvent. Monoethanolamine (MEA) is the most thoroughly researched solvent due to its quick reaction with CO_2 [27]. Figure 1.1 depicts a standard process flow diagram for a CO_2 capture plant using amine-based technology.

Typically, the plant consists of two main parts: the absorber and the desorber. The flue gas stream enters the absorber, where it mixes with the solvent, and the rich amine stream then moves to the desorber after passing through a pump and heat exchanger.

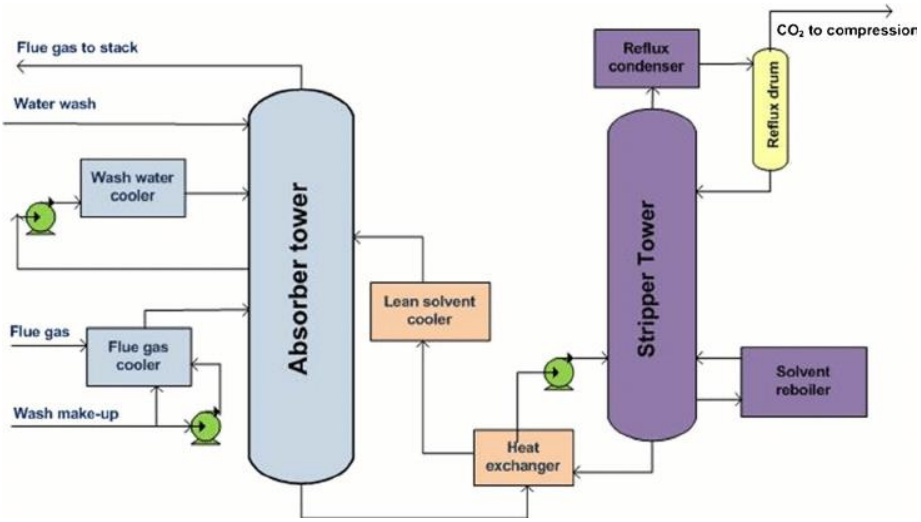

Figure 2.2: Schematic of a typical amin-based CO_2 capture plant [37].

In the desorber, CO_2 is separated from the other components of the stream using reboiler heat duty. The captured CO_2 stream exits from the top of the desorber, while the lean amine stream exits from the bottom. This lean amine stream then returns to the absorber after passing through a heat exchanger and a cooler.

2.2.1 Equipment in the amine based CO_2 capture plant

In this segment, a short explanation of the utilized equipment is given.

2.2.1.1 Absorber column

Within this column, chemical reactions and CO_2 gas absorption occur. The absorber column has two input streams: a mixture of water and solvent from the top and a flue gas stream from the bottom. Inside the column, contact devices are used to maximize the surface area between the flue gas and the liquid solvent. The pressure in the column increases from top to bottom [38].

2.2.1.2 Rich and lean amine pump

The bottom outlet stream of the absorber column, which contains a high concentration of CO_2, is pressurized by the rich amine pump to prepare it for entry into the desorber column. Similarly, the bottom outlet stream of the desorber requires a pressure boost to return to the absorber column. This is achieved by the lean amine pump, as this stream contains a lower concentration of CO_2 [38].

2.2.1.3 Lean/rich heat exchanger

Before the rich amine solution from the absorber is added to the desorption column, it must be heated. Conversely, the lean amine from the desorber needs to be cooled before entering

the absorber. To achieve this, the two streams exchange heat in a heat exchanger known as the lean/rich heat exchanger [38].

2.2.1.4 Desorber (stripper) column

In this equipment, CO_2 is separated from the amine solution using heat energy supplied by a reboiler. The captured CO_2 exits from the top of the column, while the lean solution exits from the bottom. The temperature increases from the top to the bottom of the column, while the pressure remains constant throughout [38].

2.2.1.5 Reboiler

To regenerate the amine solution, heat energy needs to be supplied to the stream containing CO_2 and the amine solution. The reboiler is the device that delivers this energy. As shown in Figure 2.6, a steam stream enters the reboiler, providing the necessary heat to the lean amine stream from the desorber [38].

2.2.1.6 Lean amine cooler

The optimal temperature for the lean amine entering the absorber is around 40°C. However, the outlet lean amine stream from the lean/rich heat exchanger has a higher temperature. Therefore, a cooler is needed to lower the temperature [38].

2.3 The Best Integrated Technology (BIT) in CCP

The CCP consortium introduced the Best Integrated Technology (BIT) to describe a power plant setup that integrates three specific measures aimed at substantially lowering the typically high costs of state-of-the-art MEA-based post-combustion capture in NGCC plants [39]. A power plant configuration developed by the CCP consortium incorporates three integration-related approaches designed to significantly reduce the power consumption of NGCC power plants. These configurations include EGR (a portion of the HRSG exhaust gas is recirculated back to the gas turbine inlet) , incorporating an amine reboiler into the HRSG, and a low-priced CO_2 capture structure that absorbs 90% of the CO_2 using a 30 weight percent of MEA (Figure 2.3). Additionally, a techno-economic analysis has been conducted to determine the optimal steam extraction spot in the steam turbine [40] [39].

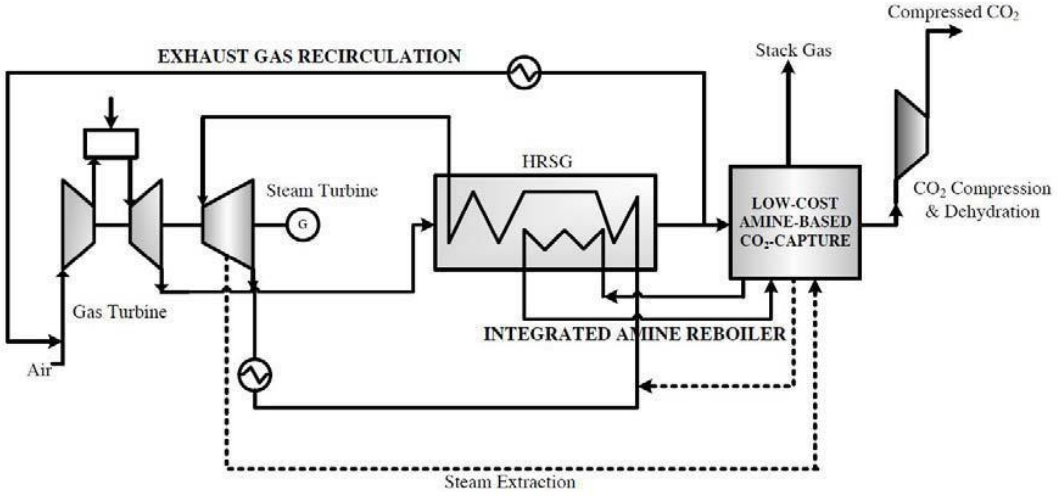

Figure 2.3: Diagram of the Best Integrated Technology (BIT) [39]

3 Simulation of the base case in Aspen HYSYS

In this study, the CO_2 capture facility and the power plant were modeled separately in Aspen HYSYS version 12, following the methodology described by Lars Erik Øi [15] and E. Abukazempour Amiri [32]. Subsequently, the two models were integrated to establish the final case, which serves as the foundation for cost analysis and optimization.

3.1 Natural gas power plant simulation

Aspen HYSYS was utilized to simulate a 400 MW natural gas combined-cycle power plant (NGCC), where natural gas is treated as pure methane. The air composition used is 79% nitrogen and 21% oxygen, with complete combustion presumed, and standard pressures and temperatures applied throughout the process. The Peng Robinson model was selected for determining the thermodynamic properties of the power plant. The essential details for the baseline simulation of the combined gas power plant using Aspen HYSYS are outlined in Table 3.1 [15].

Table 3.1: Specification and hypothesis for the base case

Parameter	Unit	Value
Inlet natural gas pressure	[bar]	30
Inlet air temperature	[°C]	25
Combustion temperature	[°C]	1500
Steam's high pressure	[bar]	120
Steam's medium pressure	[bar]	3.5
Steam's low pressure	[bar]	0.07
Stack pressure	[bar]	1.01
Stack temperature	[°C]	100

Figure 3.1 shows the PFD of NGCC in Aspen HYSYS model.

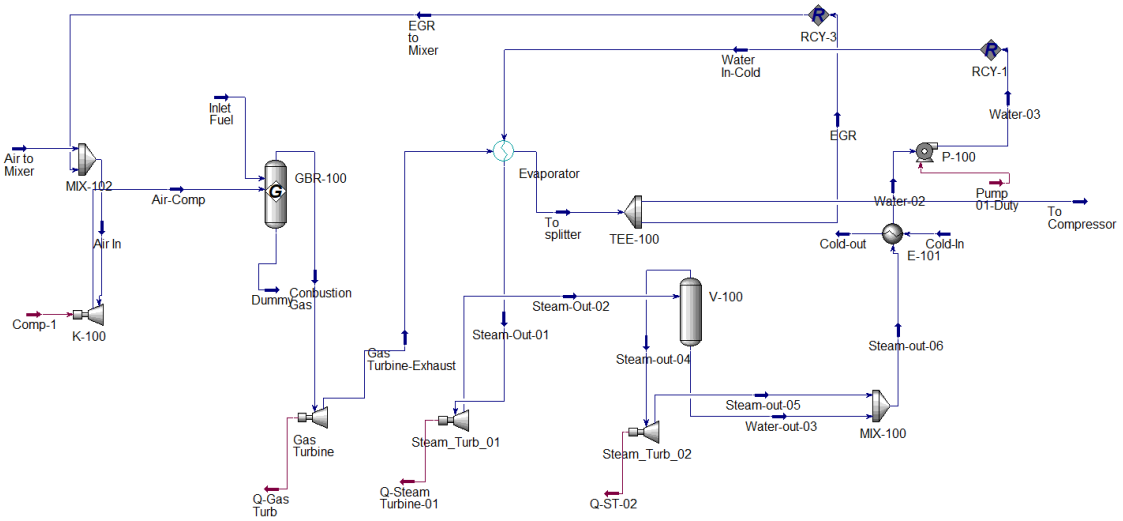

Figure 3.1: The NGCC plant modeled utilizing Aspen HYSYS

The temperature of the exhaust gas (ranging from 704 °C at the gas turbine outlet to 100 °C at the exhaust) must exceed the steam temperature across the entire steam heat exchanger to ensure the physical viability of the process.

In constructing a natural gas combined power plant, the efficiencies of the compressor, gas turbine, and steam turbine have been combined to achieve an overall thermal efficiency of 58%, aligning with industry norms. This overall efficiency is calculated by taking the net turbine output (after subtracting compressor and pump losses) and dividing it by the lower heating value of natural gas. The efficiencies of the steam turbines, gas turbine's expander, and compressor have been adjusted to 85%, 90%, and 85%, respectively, and assumed to operate adiabatically. Additionally, steam delivery for CO_2 removal is maintained at zero in this phase of the power plant simulation [15].

3.2 Simulation of CO_2 removal

A standard amine-based CO_2 capture process was modeled using Aspen HYSYS, and the outcomes of this simulation were utilized for equipment sizing and cost estimation, following the methodology outlined in previous studies [41], [42]. The input data for the simulation consisted of flue gas derived from the power plant design. The Acid Gas property package within Aspen HYSYS, which details the thermodynamics for chemical solvents, was employed for this purpose. The reactions of amine (solvent) with CO_2, included in the Acid Gas property package, are presented in Table 3.2 [43] [32].

Table 3.2: Reactions for the interaction between the MEA solvent and CO_2 in the Acid Gas property package [43]

Category	No.	Reaction	Type
Water related	(1)	$2H_2O \leftrightarrow H_3O^+ + OH^-$	Equilibrium
CO_2 related	(2)	$H_2O + HCO_3^- \leftrightarrow H_3O^+ + CO_3^{2-}$	Equilibrium
	(3)	$CO_2 + OH^- \rightarrow HCO_3^-$	Kinetic
	(4)	$HCO_3^- \rightarrow CO_2 + OH^-$	Kinetic
MEA related $HO(CH_2)_2NH_2$	(5)	$HO(CH_2)_2H^+NH_2 + H_2O \leftrightarrow HO(CH_2)_2NH_2 + H_3O^+$	Equilibrium
	(6)	$HO(CH_2)_2NH_2 + H_2O + CO_2 \rightarrow HO(CH_2)_2NHCOO^- + H_3O^+$	Kinetic
	(7)	$HO(CH_2)_2NHCOO^- + H_3O^+ \rightarrow HO(CH_2)_2NH_2 + H_2O + CO_2$	Kinetic

The absorber and desorber were modeled using equilibrium stages with specific Murphree efficiency values determined by the user. A constant Murphree efficiency of 0.25 for the absorber and 1.00 for the desorber was found to be the same to one meter of structured packing in each unit, respectively. These efficiencies are calculated by measuring the change in CO_2 mole ratio across the stages against the shift assumed in equilibrium conditions [18].

The calculation details, which include an 90% CO_2 removal efficiency and a ΔT_{min} of 10 °C in the lean/rich amine heat exchanger, are outlined in Table 3.3. The method of computation follows the same approach as used in previous studies [41], [44], [45].

Table 3.3: Aspen HYSYS model's parameters and conditions [15]

Item	Property	Unit	Value
Inlet Flue Gas	Pressure	[bar]	1.1
	Temperature	[°C]	40
	Molar flow rate	[kmol/h]	85000
	CO_2 content	[mole %]	3.73
	H_2O content	[mole %]	6.71
Lean MEA	Pressure	[bar]	1.1
	Temperature	[°C]	40
	Molar flow rate	[kmol/h]	120000 (Note)
	Concentration of MEA	[weight %]	29
	CO_2 content	[weight %]	5.5

Absorber	Number of stages	-	10
	Murphree eff.	[%]	25
	Pump pressure of rich amine	[bar]	2
	Temperature output of lean/rich amine HEX (For rich amine)	[°C]	104.5 (Note)
Desorber	Number of stages in the stripper	-	6
	Murphree eff.	[%]	100
	Reflux ratio in the desorber	[%]	30
	Temperature of reboiler	[°C]	120
	Pressure	[bar]	2
	Pump pressure of lean amine	[bar]	5
Note): Value of the initial iteration			

Process flow diagram for the CO_2 removal simulation in Aspen HYSYS is shown in Figure 3.2. The absorption column's initial calculations are based on the flue gas and lean amine input data [45]. Rich amine is pumped from the bottom of the absorption column into the lean/rich amine heat exchanger. Following the absorber and rich pump, there is a slight increase in temperature before the duty of the heat exchanger is determined based on the projected output temperature from the lean/rich amine heat exchanger. As the warmed rich amine enters the desorption column, the CO_2 product and the hot lean amine are computed at the output. The hot lean amine is then pressurized by the lean amine pump, routed through the lean/rich heat exchanger for cooling, and subsequently cooled further in the lean amine cooler. The cooled lean amine is introduced into a recycling loop. The process assesses whether the flow and condition of the recycled lean amine match the previously calculated flow and may adjust through iteration. The recycling block in Aspen HYSYS compares the block's input to its output in the final iteration to resolve the flowsheet [46].

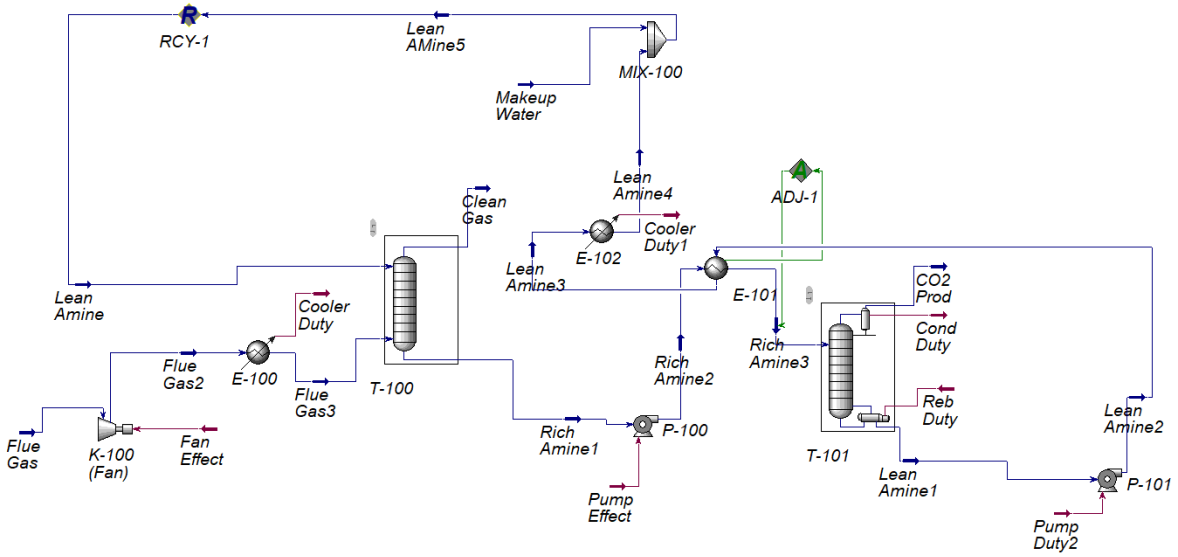

Figure 3.2: A simplified Aspen HYSYS flow sheet model for CO_2 removal

3.3 Simulation of the base case

In the subsections mentioned earlier, the natural gas power plant and the CO_2 capture plant are integrated, culminating in the final base case simulation. The flue gas from the natural gas power plant is directed into the CO_2 capture facility. This simulation in Aspen HYSYS aims to achieve a net electricity output of 400 MW and 90% CO_2 removal efficiency. While the overarching concept remains consistent with previous models, a key difference in this new simulation is that the volume of flue gas fed into the CO_2 removal plant is determined by the output from the combined cycle power plant.

In this updated simulation, certain specifications have been altered based on the exhaust gas characteristics of the cycle power plant. Table 3.4 outlines the revised specification data for the base case simulation, which includes generating 400 MW, achieving a combustion chamber exhaust temperature of 1500 °C, removing 90% of CO_2, ΔT_{min} of 10 °C in the lean/rich amine heat exchanger, and setting the input flue gas temperature to the absorber at 40 °C and setting 75 °C as the ΔT_{min} in the evaporator.

Table 3.4: Aspen HYSYS specifications for base case model

Item	Property	Unit	Value
Inlet Flue Gas	Pressure	[bar]	1.1
	Temperature	[°C]	40
	Molar flow rate	[kmol/h]	71345

	CO_2 content	[mole %]	4.61
	H_2O content	[mole %]	6.71
Lean MEA	Pressure	[bar]	1.1
	Temperature	[°C]	40
	Molar flow rate	[kmol/h]	99496
	Concentration of MEA	[Weight	28.92
	CO_2 content	[Weight	5.39
Absorber	Number of stages	-	10
	Murphree eff.	[%]	25
	Pump pressure of rich amine	[bar]	2
	Temperature output of lean/rich amine HEX	[°C]	102.7
Desorber	Number of stages in the stripper	-	6
	Murphree eff.	[%]	100
	Reflux ratio in the desorber	[%]	30
	Temperature of reboiler	[°C]	120
	Pressure	[bar]	2
	Pump pressure of lean amine	[bar]	5

PFD for the base case simulation in Aspen HYSYS, with each fluid stream labeled to identify its destination in subsequent equipment is shown in Figure 3.3.

To meet the simulation requirements and facilitate the design of an automated simulation model, six adjustment operations have been incorporated. The combustion temperature is regulated by the air input flow rate using ADJ-1. The net electricity output is determined by the natural gas flow rate with ADJ-2. The minimum approach temperature in evaporator is controlled by ADJ-3.

ADJ-4 alters the cooling water requirement in the inlet cooler to modify the flue gas temperature to the absorber.The minimum approach temperature in the lean/rich heat exchanger is controlled by the rich amine outlet temperature using ADJ-5. Finally, The CO_2 removal efficiency is adapted based on the flow rate of lean amine using ADJ-6.

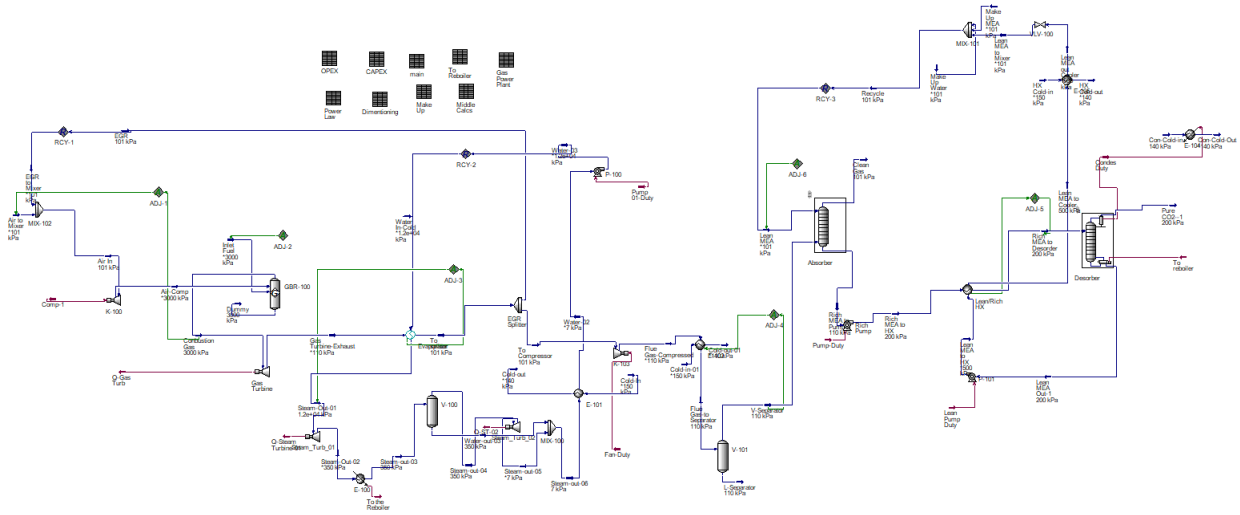

Figure 3.3: Aspen HYSYS flow sheet model for the base case

To enhance the simulation's efficiency, three additional recycling blocks have been implemented. The first one is used for exhaust gas recycling process. RCY-2 is used for the water recycling process in the steam turbine, and RCY-3 is lean amine recirculation process line. The process also addresses shortages in amine solution and water. To compensate for these deficiencies, makeup streams are introduced into the primary flows. A spreadsheet was created to manage these makeup streams, calculating the necessary amounts of water and amine solution based on mass balance equations. These amounts are then integrated into the system as mass flows to the makeup amine solution as well as makeup water streams. Prior to entering the absorber, an inlet cooler, a fan unit, and a separator are employed to achieve the desired temperature and pressure of the entering flue gas to the absorber and to separate water from the flue gas.

At the end, the process is simulated and the duty in the reboiler is stabilized at some value and the results are given in chapter seven. Also, the results show that, the key value of reboiler duty per kilo of CO_2 removed is 4.5 MJoule/kg CO_2 which is in the acceptable range.

4 Equipment dimensioning

In this segment, the dimensioning of process equipment relevant to the base case's process simulation is outlined. Estimates are derived from the outcomes of the base case simulation's process flowsheet, encompassing factors such as flow rates, temperatures and heat/power duties. While Aspen HYSYS outputs are displayed in the tables, other values are either calculated or assumed. The calculations and assumptions utilized for sizing are partially presented in the tables. Only key equipment pieces, like compressors, gas turbine, steam turbines, absorption, desorption columns, evaporators, condensers, heat exchangers, pumps, fans and separators, are sized. This section excludes considerations for pre-treatments such as inlet gas purification or post-treatments for example CO_2 compression, transport, or storage.

The Aspen Icarus Reference Guide serves as the authoritative source for sizing the equipment mentioned [47].

4.1 Gas turbine with combustion chamber

The gas turbine's design hinges on its power output, a crucial parameter. Utilizing the defined power output design outlined in the Aspen Icarus Reference Guide [47], alongside the power output data from Aspen HYSYS, the following sizing is conducted. Table 4.1 illustrates the gas turbine's sizing according to the demands of the base case simulation. In this scenario, the maximum power output feasible for consideration is 375,000 KW. With the required power output in mind, two gas turbines are necessary.

Table 4.1: Parameters of gas turbine dimensioning

Parameter	Unit	Value
Power output	[KW]	596200
Power output (Max per unit)	[KW]	375000
Computed No. of units	-	1.59
Actual No. of units	-	2.00
Power output (Per unit)	[KW]	298100

4.2 Steam Turbine

The primary design consideration for a steam turbine is its power generation capacity. The performance and sizing details of the steam turbines are displayed in Table 4.2.

Table 4.2: Parameters of steam turbines dimensioning

Parameter	Unit	Steam turbine No.1 (High Pressure)	Steam turbine No.2 (Low Pressure)
Power output	[KW]	87100	20720
Power output (Max per unit)	[KW]	22,300	22300
Computed No. of units	-	3.906	0.9292
Actual No. of units	-	4.00	1.00
Power output (Per unit)	[KW]	21780	20720

In this scenario, the highest achievable power output of a non-condensing type steam turbine stands at 22,300 KW [47]. Given the required power output, four high-pressure steam turbines and two low-pressure steam turbines are needed.

4.3 Evaporator

The primary determinant in designing the cost of heat exchangers is typically the surface area available for heat transfer. In determining the necessary heat transfer level within the evaporator, a specified overall heat transfer coefficient of 0.25 KW/m2°K is utilized [48]. The exhaust output from the gas turbine expander, at a temperature of 704 ℃, serves as the input parameter and heat source for evaporating water, subsequently employed in the steam turbine. In the base case scenario, it is presumed that the evaporator maintains a minimum temperature approach of 75 ℃, consequently ensuring that the flue gas output from the evaporator remains at a temperature of 100 ℃ [15].

In this sizing, the long tube vertical evaporator with a highest heat transfer area of 4640 m2 is designated [47]. Considering the total required heat transfer in the simulation, four evaporators are included. Table 4.3 illustrates the primary sizing parameters and the computed duty derived from Aspen HYSYS.

Table 4.3: Dimensioning values of the evaporator

Parameter	Unit	Value
Duty	[KJ/h]	1442000000
Heat transfer coefficient	[KW/m^2°K]	0.25
LMTD	[°C]	104
Total heat transfer area	[m^2]	15400
Area (Max per unit)	[m^2]	4640
Computed the No. of units	-	3.319
Actual No. of units	-	4.00
Actual area (Per unit)	[m^2]	3850

4.4 Condenser

In the steam turbine cycle, the process water needs to transition from vapor to liquid phase for reuse. To facilitate this transition before reaching the pump, the condenser is considered. The crucial design parameter for the condenser is the actual volume flow rate of cooling water [32]. The sizing of the compressor, based on this defined design parameter, is presented in Table 4.4.

Table 4.4: Dimensioning values of the condenser

Parameter	Unit	Value
Water flow rate in hour	[m^3/h]	10620
Water flow rate in second	[litter/s]	2950
Water flow rate (Max)	[litter/s	315
Computed the No. of units	-	9.366
Actual No. of units	-	10
Actual water flow rate	[litter/s]	295

For the dimensioning of the base case simulation, a barometric condenser with 315 litter/s as the maximum actual water flow rate at the inlet, is specified [47]. Considering the required actual water flow rate, ten condensers are included in the sizing process.

4.5 Compressor

The primary effective parameter in the compressor design, is the actual inlet gas flow rate [32]. The sizing of the compressor, according to the specified design parameters, is shown in Table 4.5.

Table 4.5: Dimensioning values of the compressor

Parameter	Unit	Value
Flow rate	[m^3/h]	1714000
Flow rate (Max)	[m^3/h]	509700
Computed No. of units	-	3.336
Actual No. of units	-	4.00
Computed flow rate	[m^3/h]	428529.5

For the base case simulation dimensioning, a centrifugal gas compressor paired with a driver

(turbine, motor or gasoline-driven engine) is designated, capable of handling a maximum actual gas flow rate at the inlet of 509,700 m^3/h [47]. Dimensioning considers four compressors based on the necessary actual gas flow rate.

4.6 Absorber

Table 4.6 displays the performance and sizing details of the absorber column. The absorber's CO_2 removal rate, set at 90%, is primarily adjusted by the flow rate of lean amine within the parameters of the base scenario.

Table 4.6: Dimensioning values of the absorber

Parameter	Unit	Value
Exhaust gas volumetric flow rate	[m^3/h]	1809000
Exhaust gas volumetric flow rate	[m^3/s]	502.4
Exhaust gas velocity	[m/s]	2.5
Inner diameter	[m]	16
Height of column	[m]	25
Height of packing	[m]	10
Volume of column	[m^3]	5024
Volume of packing	[m^3]	2010
No. of units	-	3
Column volume (Per unit)	[m^3]	1674
Packing volume (Per unit)	[m^3]	669.8
Diameter (Per unit)	[m]	9.235
Shell material	-	SS316
Packing type	-	MellaPak 250Y

The vertical flue gas velocity within the packed column is set at 2.5 m/s, derived from 75% of the flooding velocity of Mellapak 250Y structured packing types [49]. Considering this gas velocity and the high-volume flow rate of flue gas, three absorbers are taken into consideration, leading to a diameter of 9.235 m per unit for the absorber column. The total height of the absorption columns is estimated to be 25 meters. Various factors such as packaging, gas inflow and outflow, liquid distributors, water wash, and demister are all taken into account when calculating the height of the absorber [32].

4.7 Desorber

Table 4.7 presents the performance and design attributes of the desorber column.

Table 4.7: Dimensioning values of the desorber

Parameter	Unit	Value
Fluid volume flow	[m^3/h]	134800
Fluid volume flow	[m^3/s]	37.44
Fluid velocity	[m/s]	1.00
Inner diameter	[m]	6.9
Height of column	[m]	15
Height of packing	[m]	6
Volume of column	[m^3]	561.7
Volume of packing	[m^3]	224.7
No. of units	-	1
Shell material	-	SS316
Packing type	-	MellaPak 250Y

Kallevik's master thesis was referenced to compute the vertical gas velocity within the column [46]. The result led to a column diameter of 6.9 meters. It is anticipated that the column will have a total height of 15 meters, comprising 6 meters of the structured packing. A Murphree stage efficiency of 100% per meter is assumed for the column.

4.8 Heat exchangers

This section furnishes details on the operation and sizing of various components including lean MEA cooler, inlet cooler, lean/rich heat exchangers, reboiler and condenser. Employing a calculation scheme akin to other sections, it is assumed that all heat exchangers are of the shell and tube type lean/rich heat exchanger.

Table 4.8 showcases the identified duty from Aspen HYSYS alongside the crucial dimensioning parameters for a lean/rich heat exchanger. The overall heat transfer coefficients for the lean/rich heat exchanger were set at 732 W/ (m2. K) [50] [32]. The logarithmic mean temperature difference (LMTD) is computed with ΔT_{min} set to 10°C. Using the computed heat duty, the total heat transfer area is found out. Based on this maximum area and total area of each heat exchanger unit, it is determined that 29 heat exchanger units are required, with each unit's actual area calculated to be 985.

Table 4.8: Dimensioning values of the Lean/rich heat exchanger

Parameter	Unit	Value
Duty	[KJ/h]	777200000
Heat transfer Coeff.	[kW/m^2. K]	0.732
LMTD	[°C]	10.33
Total heat transfer area	[m^2]	28560
Area (Max per unit)	[m^2]	1000
Computed the No. of units	-	28.56
Actual No. of units	-	29
Actual area (Per unit)	[m^2]	985

4.8.1 Lean MEA cooler

Table 4.9 presents the identified duty from Aspen HYSYS along with the essential dimensioning parameters for the lean MEA cooler.

Table 4.9: Dimensioning values of the Lean MEA cooler

Parameter	Unit	Value
Duty	[KJ/h]	269700000
Heat transfer Coeff.	[kW/m^2. K]	0.8
LMTD	[°C]	29.36
Total heat transfer area	[m^2]	3189
Area (Max per unit)	[m^2]	1000
Computed No. of units	-	3.189
Actual No. of units	-	4
Actual area (Per unit)	[m^2]	797.4

Regarding lean MEA cooler, the overall heat transfer coefficients were set at 800 W/ (m2. K) [50]. The minimum temperatures of the cold and hot sides of the lean MEA cooler are employed to compute the LMTD. Utilizing the obtained heat duty, the total heat transfer area is calculated. Based on this maximum area and total area of each lean MEA unit, it is determined that four lean MEA cooler units are needed, with each unit's actual area calculated as 797.4.

4.8.2 Inlet cooler

The inlet coolers were configured with an overall heat transfer coefficient of 800 W/ (m2. K) [50]. The LMTD is computed using the minimum temperatures of the hot and cold sides of the inlet cooler. Utilizing the obtained heat duty, the total heat transfer area is established. Based on this maximum area and the total area the of each inlet cooler unit, it is concluded that two inlet cooler units are required, with each unit's actual area calculated as 841 m^2.

Table 4.10 presents the performance of the inlet cooler and its dimensioning results.

Table 4.10: Dimensioning values of the inlet cooler

Parameter	Unit	Value
Duty	[KJ/h]	239900000
Heat transfer Coeff.	[kW/m^2. K]	0.8
LMTD	[°C]	49.50
Total heat transfer area	[m^2]	1683
Area (Max per unit)	[m^2]	1000
Computed No. of units	-	1.683
Actual No. of units	-	2
Actual area (Per unit)	[m^2]	841

4.8.3 Reboiler (For desorber)

The reboiler duty is determined through calculations performed by Aspen HYSYS. The LMDT is computed based on the temperatures of the cold and hot sides of the reboiler. The overall heat transfer coefficient (U), obtained from literature, is assumed to remain constant at 1200 W/ (m2. K) [50]. Utilizing the heat exchanger equation, the total needed heat exchanger area is calculated to be 5767 m2. Considering the the maximum area and total heat transfer area of each reboiler unit, it is determined that six reboiler units are necessary, with each unit's actual area calculated as 961.1 m^2.

Table 4.11 illustrates the computations and operational characteristics of the boiler used in the desorber.

Table 4.11: Dimensioning values of the reboiler

Parameter	Unit	Value
Duty	[KJ/h]	595500000
Heat transfer Coeff.	[Kw/m2.	1.20
LMTD	[°C]	23.90
Total heat transfer area	[m2]	5767

Temp out-cold	[°C]	120
Temp in-cold	[°C]	114.9
Temp in-hot	[°C]	143.9
Temp out-hot	[°C]	138.8
Area (Max per unit)	[m2]	1000
Calculated No. of units	-	5.767
Actual No. of units	-	6
Actual area (Per unit)	[m2]	961.1

4.8.4 Condenser (For desorber)

Table 4.12 illustrates the computations and operational characteristics of the condenser employed in the desorber.

Table 4.12: Dimensioning values of the condenser

Parameter	Unit	Value
Duty	[KJ/h]	70710000
Heat transfer Coeff.	[kW/m^2. K]	1.00
LMTD	[°C]	81.02
Total heat transfer area	[m^2]	242.4
Temp out-cold	[°C]	25
Temp in-cold	[°C]	15
Temp in-hot	[°C]	104.3
Temp out-hot	[°C]	97.75
Area (Max per unit)	[m^2]	1000
Computed No. of units	-	0.2424
Actual No. of units	-	1
Actual area (Per unit)	[m^2]	242.4

The condenser duty is determined through calculations performed by Aspen HYSYS. The LMTD is computed based on the temperatures of the hot and cold sides of the condenser. The overall heat transfer coefficient (U), obtained from literature, is assumed to remain fix at 1000 W/ (m2. K) [50]. Utilizing the heat exchanger formulas, the total needed heat exchanger area is figured to be 242.4 m^2, requiring one condenser unit.

4.9 Pumps and fan

This section addresses the dimensions taken into account for the water pump, lean pump, and rich pump as well as the fan. The pumps and fan in Aspen HYSYS are engineered to attain an adiabatic efficiency of 75%. While the duty serves as a sizing principle for the pumps and fan obtained from Aspen HYSYS, the Aspen In-Plant cost calculator employs volumetric flow to determine equipment costs [32].

4.9.1 Rich amine pump

Transferring the rich amine solvent to the desorber is crucial. The desorber operates at a pressure of 2 bars, following the rich amine pump. The Aspen HYSYS values for the rich amine pump are provided in Table 4.13.

Table 4.13: Dimensioning values of the rich amine pump

Parameter	Unit	Value
Power	[KW]	132.9
Flow rate (In hour)	[m^3/h]	3988
Flow rate (In second)	[L/s]	1108
Actual No. of units	-	1.00

According to the flow rate calculated by Aspen HYSYS, a centrifugal pump is selected for this process [47], and based on the pump's specifications, one unit is deemed sufficient for this design.

4.9.2 Lean amine pump

Following the desorber, a pump is required to raise the solution to the absorber's height, requiring increased power consumption to achieve the necessary lift. Installing a lean amine pump elevates the pressure of the lean amine to 5 bar. The Aspen HYSYS computation details for the rich amine pump are outlined in Table 4.14.

A centrifugal pump is designated for this process [47], determined by the flow rate estimated by Aspen HYSYS, and one pump is deemed adequate for this design.

Table 4.14: Dimensioning values of the Lean amine pump

Parameter	Unit	Value
Power	[kW]	459.2
Flow rate (In hour)	[m^3/h]	4133
Flow rate (In second)	[L/s]	1148
Actual No. of units	-	1

4.9.3 Water pump

After the condenser and before the evaporator, a water pump is contemplated to circulate the condensed water for using again in the steam turbine. The details of the Aspen HYSYS calculation for the water pump are presented in Table 4.15.

Table 4.15: Dimensioning values of the water pump

Parameter	Unit	Value
Power	[kW]	1859
Flow rate (In hour)	[m^3/h]	419.8
Flow rate (In second)	[L/s]	116.6
Actual No. of units	-	1

According to the anticipated flow rate determined by Aspen HYSYS, a centrifugal pump is selected for this process [44], and one unit of the pump is deemed sufficient for this design.

4.9.4 Flue gas fan

Table 4.16 shows the flue gas fan's output dimensioning parameters from Aspen HYSYS

Table 4.16: Dimensioning values of the Flue gas fan

Parameter	Unit	Value
Power	[kW]	7255
Flow rate	[m^3/h]	2245000
Max flow rate	[m^3/h]	1529000
Computed No. of units	-	1.468
Actual No. of units	-	2.00
Actual flow rate	[m^3/h]	1123000
Actual power (Per unit)	[kW]	3627

As previously stated, the actual flow rate is the primary design parameter for a flue gas fan. A centrifugal fan using a maximum actual flow rate of 1,529,000 m3/h is designated for the dimensioning process [47]. Based on the calculated actual flue gas flow rate, two fans are necessary in the sizing.

4.10 Separators

The heat required for the reboiler in the desorber is provided by the steam outlet from the first steam turbine. As a result of this heat transfer, some of the steam condenses into water, which needs to be separated before entering the second steam turbine.

Additionally, before the flue gas enters the absorber, a small amount of water might be present due to the temperature decrease in the inlet cooler. If this water is extracted from the flue gas in the separator, the flue gas can enter the absorption column at approximately 40°C.

4.10.1 Separator No.1

Table 4.17 showcases the water separator utilized to segregate liquid water from steam. The separator's diameter was determined using the Souders–Brown equation, resulting in a calculation for a vertical vessel with a k-factor of 0.107 m/s and a tangent-to-tangent diameter ratio of 1 [46]. Also, for cost estimation purposes, the vessel volume is considered in this scenario.

Table 4.17: Dimensioning values of the separator No.1

Parameter	Unit	Value
Actual gas flow rate (In hour)	[m^3/h]	80200
Actual gas flow rate (In second)	[m^3/s]	22.28
Density of liquid phase	[kg/m^3]	914
Density of gas phase	[kg/m^3]	1.884
Vapour velocity (Allowable)	[m/s]	2.354
Cross-sectional area	[m^2]	9.463
Inner-diameter	[m]	3.471
Height	[m]	10.44
Volume	[m^3]	98.8
Sounder-Brown velocity (K factor)	-	0.107

4.10.2 Separator No.2

Table 4.18 presents the water separator employed for segregating liquid water from flue gas.

Table 4.18: Dimensioning values of the separator No.2

Parameter	Unit	Value
Actual gas flow rate (In hour)	[m^3/h]	1686000
Actual gas flow rate (In second)	[m^3/s]	468.5
Density of liquid phase	[kg/m^3]	996
Density of gas phase	[kg/m^3]	1.207
Sounder-Brown velocity (K factor)	-	0.15
Vapour velocity (Allowable)	[m/s]	4.306
Cross sectional area	[m^2]	108.8

Inner diameter	[m]	11.77
Height	[m]	35.34
Volume	[m^3]	3844

The separator's diameter was calculated via the Souders-Brown equation, resulting in a vertical vessel with a diameter-to-tangent ratio of 1 and a k-factor of 0.15 m/s [46]. Furthermore, in this instance, vessel volume is utilized to assess costs.

4.11 Dimensioning summary

The summary of dimensioning parameters are shown in Table 4.19.

Table 4.19: Summary of dimensioning parameters and values

Equipment	Dimensioning parameter	Unit	Value
Gas Turbine with C-C	Power output per unit	[KW]	298100
Steam Turbine 1	Power output per unit (KW)	[KW]	21780
Steam Turbine 2	Power output per unit	[KW]	20720
Compressor	Calculated flow rate	[m3/h]	428529.5
Water Pump	Flow rate	[L/s]	116.6
Evaporator	Actual area per unit	[m2]	3850
Condenser	Actual area per unit	[m2]	242.4
Separator-1	Vessel volume	[m3]	98.8
Absorber	Column volume per unit	[m3]	1674
Desorber	Column volume	[m3]	561.7
Lean/rich HEX	Actual area per unit	[m2]	985
Lean MEA Cooler	Actual area per unit	[m2]	797.4
Reboiler-D	Actual area per unit	[m2]	961.1
Inlet Cooler	Actual area per unit	[m2]	841
Condenser-D	Actual area per unit	[m2]	242.4
Fan	Actual flow rate	[m3/h]	1123000
Lean Pump	Flow rate	[L/s]	1148
Rich Pump	Flow rate	[L/s]	1108
Separator-2	Vessel volume	[m3]	3844

5 Cost estimation

The main objective of cost estimation in this chapter is to figure out the total cost of the project, which encompasses both the combined cycle power plant and the CO_2 capture plant. The cost estimation computations are based on the dimensions derived from the Aspen HYSYS results. The Aspen In-Plant Cost Estimator is used to calculate the costs for each piece of equipment in the base case model.

Below is the procedure utilized to estimate the total cost of the plant based on the results of the model:

i. Costs of items are calculated using the dimensioning data from the base case, via Aspen In-Plant Cost Estimator (v.12).
ii. The overall installation cost is specified using the Enhanced Detailed Factor (EDF).
iii. Cost index correction is applied to determine the present value (adjusted to the current year).
iv. Annual OPEX are calculated.
v. NPV is calculated using a designated discount rate and the expected life of the plant.
vi. Costs are adjusted for parameter changes using the power law method

5.1 Capital expenditure (CAPEX)

In this study, the 12th version of the Aspen In-Plant Cost Estimator was used to determine the CAPEX. Additionally, the capital cost was calculated using the Enhanced Detail Factor (EDF) method. This method considers various factors that affect the installation of each piece of process equipment. The EDF approach has enabled the optimization of specific pieces of equipment and has facilitated techno-economic analysis for the development of both existing process plants and new technologies [51].

5.1.1 Cost of equipment

The Aspen In-Plant, a software designed for cost estimation that integrates process information, dimensioning factors, and materials, was employed to generate accurate cost estimates for each piece of equipment. Aspen In-Plant set default values for other specifications, except for the dimensioning factors discussed in the previous chapter. It provided prices in Euro (€) for the year 2019. Also, it takes Rotterdam, Netherlands, as the default place.

In Appendix B, the detailed installation factor table by Nils Henrik Eldrup includes parameters specifically for carbon steel (C.S.). While most of the equipment is made of stainless steel,

some are made from C.S. To use Nils' detailed installation factor, the cost of stainless steel should be converted to the cost of carbon steel using a material factor according to the EDF method [51]. This has been done through equation (5.1).

$$Equipment\ Cost_{CS} = \frac{Equipment\ Cost_{SS}}{f_{mat}} \tag{5.1}$$

whereas:

- $Cost_{CS}$ = Cost of equipment which its material is carbon steel (C.S).
- $Cost_{SS}$ = Cost of equipment which its material is stainless steel (S.S).
- f_{mat} = Material factor to convert S.S into C.S.

To adjust prices for rotating and welded items from SS316 to CS is, the value of f_{mat} is 1.30 and 1.75, correspondingly [41].

5.1.2 Total installation cost

The total cost of the plant can be calculated using the equipment costs listed in the table of installation factors for 2020 found in Appendix B. This table includes not only the direct costs but also covers engineering, administration, commissioning, and contingency expenses.

Using equation (5.2) can be used for calculation of the total installation cost based on the purchase price of each equipment item [32].

$$C_i = C_p \left[f_{tc} - f_p - f_E + f_m * \left(f_p + f_E \right) \right] \tag{5.2}$$

Whereas:

- C_i = Total installed cost- for carbon steel [Euros]
- C_P = Equipment purchase cost- for carbon steel [Euros]
- f_{TC} = Total installation cost factor
- f_P = Equipment piping cost factor
- f_E = Equipment cost factor
- f_m = Material cost factor

5.1.3 Inflation and currency parameters

All cost calculations in this project are conducted in Euros (€). The Aspen In-Plant cost calculator is utilized to determine the cost of equipment in euros, and the factor table for the EDF approach also specifies the currency of equipment costs in euros [41].

The 12_{th} version of the Aspen In-Plant cost estimator, which uses data from 2019, requires updating for inflation to provide a current and accurate cost estimate. The data for calculating the installed cost factors from the detailed factor table pertains to the year 2020. Therefore, equipment costs must first be adjusted to 2020 costs. Subsequently, the total installation cost

will be estimated using the EDF method. Finally, inflation adjustments need to be applied to the overall installed costs from 2020 to the present year.

The price has been transferred from year a to year b applying equation (5.3):

$$Cost_a = Cost_b \left(\frac{Cost\ Index_a}{Cost\ Index_b}\right) \tag{5.3}$$

The cost indexes for the current work are transcribed in Table 5.1:

Table 5.1: Cost inflation indexes from 2019 to 2023 [49]

Year	Cost inflation-index
2019	110.1
2020	112.2
2021	116.1
2022	122.8
2023	129.8

All the methods for calculating the CAPEX for the base case, are included in Aspen HYSYS spreadsheet.

5.1.4 Power Law

As the calculated costs in Aspen In-Plant are for a base capacity of each equipment, there is a need to modified these costs to the actual capacity of each equipment. This is done by the use of power law. The power law capacity correlation is shown in equation (5.4) [53]:

$$C_E = C_B \left(\frac{Q}{Q_B}\right)^M \tag{5.4}$$

here, Q and Q_B represent the actual capacity and base capacity of the equipment, respectively. C_B is also the cost of an equipment with the capacity of Q_B.

For the scaling constant (M), although the valve is between 0.4 and 0.9 but it is usually considered 0.65.

5.2 Operating expenditure (OPEX)

In addition to CAPEX, OPEX must also be assessed for comprehensive cost estimation. The OPEX costs factored into this project include maintenance expenses, electricity costs, MEA

costs, steam costs, and the salaries of the engineers and operators involved in the project. Equation (5.5) is utilized to calculate the annual cost of the utilities provided [51].

$$\text{Anual utility cost} = \text{Consumption} \times \frac{\text{Operating hours}}{\text{year}} \times \text{Utility price} \quad (5.5)$$

Table 5.2 gives the OPEX descriptions and assumptions [41], [50], [54].

Table 5.2: OPEX parameters and values

Item	Unit	Value
Project's life duration	[Year]	25
Operation's duration	[Year]	22
Construction's duration	[Year]	3
Discount rate	[%]	7.5
Project's operating hours	[h/year]	8000
Electricity price	[€/kWh]	0.09
Natural gas price	[€/m3]	1.29
Cooling water price	[€/m3]	0.022
Process water price	[€/m3]	0.203
Solvent (MEA) price	[€/ton]	1450
Maintenance cost	[€/year]	4% of the CAPEX
No. of operators	[Person]	12
No. of engineers	[Person]	2
Operator wage and cost	[€/year]	80414 × 12
Engineer wage and cost	[€/year]	156650 × 2

All the procedures required to calculate the OPEX for the base case were included in a spreadsheet labeled "OPEX" within the Aspen HYSYS simulation.

5.3 Revenue from electricity sales

In this project, generating and selling electricity from both the gas turbine and steam turbine at the combined power plant is economically beneficial, and this income is included in the cost calculations. The electrical output is consistently set at 400 MW in all scenarios under consideration. The electricity is sold at €0.09 per kWh, which mirrors the average rate in 2023. Although electricity prices could increase in the coming years, they are projected to stay stable

throughout the life of the project. The average monthly wholesale electricity price in Norway from january 2019 to march 2024 is shown in Figure 5.1 [54].

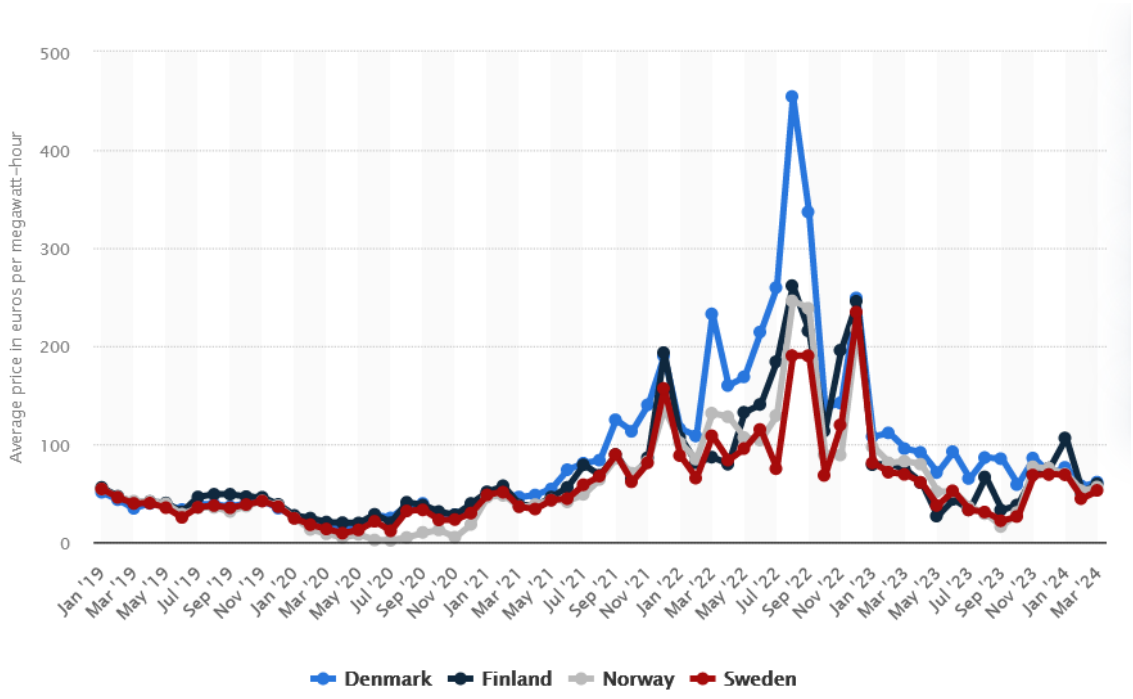

Figure 5.1: Average monthly electricity wholesale fee in the Nordic countries (Jan-2019 to Mar-2024) [54]

5.4 Net present value (NPV)

The overall cost of the project can be assessed over time by considering both the capital expenses involved in setting up the necessary equipment and the operational utility costs. The total project cost is calculated using the net present value (NPV) method, which takes into account both capital and operational expenses, revenue over the specified period, and the discount rate. In this calculation, the capital expenses include all costs associated with installing the main components at the combined power plant and the CO_2 capture facility.

The capital expenditures (CAPEX) are expected to occur from year 0 to year 2, whereas the operational costs and revenues will occur after this period. Equation (5.6) represents the formula used to calculate the net present value (NPV) of the total future operational costs [46].

$$NPV_{Opex} = \sum_{N=3}^{END} \left\{ a \times \frac{1}{(1+i)^N} \right\} \tag{5.6}$$

Where:

- NPV_{OPEX} = The total OPEX for the entire period [Euro]
- N = Number of years
- a = Annual operation cost [Euro]

- i = Annual interest rate

Equation (5.7) is utilized to calculate the net present value (NPV) for the entire process in this study.

$$NPV = CAPEX + NPV_{OPEX} \tag{5.7}$$

Whereas:

- NPV= Net present value [Euro]
- CAPEX = Equipment installation expenses [Euro]

Equation (5.7) takes into account all revenues and costs associated with the utilities as well as the CAPEX when calculating the NPV. Initially, the NPV is negative in the early years but becomes positive later, influenced by the revenue from electricity sales. A higher NPV suggests greater profitability of the project. As mentioned earlier, the project is evaluated over a 25-year period with a discount rate of 7.5%.

6 Sensitivity analysis

This chapter examines the effects of altering key process parameters to achieve the best balance for a gas-based power plant combined with a CO_2 capture system. The optimization of this process is guided by an economic assessment aimed at maximizing profits over a specific time frame.

Several factors influence the net present value (NPV) of a power plant, such as the Exhaust Gas Recirculation (EGR) rate and the minimum temperature difference in the evaporator. In the CO_2 capture facility, NPV is also affected by variables like the minimum temperature difference in the lean/rich heat exchanger. Additionally, other parameters like the inlet air/gas temperature and pressure entering the power plant, the outlet temperature of the flue gas, and the packing height in the absorption column could also be considered. However, since these have been previously examined in the Aboukazempour Amiri thesis [32], they are not included in this sensitivity analysis.

The main goal of this research is to utilize Aspen HYSYS for estimating and optimizing various parameters to maximize the net present value (NPV) of the combined gas power plant with an integrated CO_2 capture system. The process for calculating NPV includes several steps: initially, the CAPEX and OPEX are determined for the base case. Following parameter adjustments, the updated dimensioning parameters are transferred from the dimensioning spreadsheet to the power law spreadsheet to recalculate the CAPEX. Simultaneously, the operational costs are automatically updated in the OPEX spreadsheet based on changes in utility usage. Additionally, revenue from electricity sales is factored into the NPV calculation.

In terms of sensitivity method, all sensitivities were done by automatic calculation with HYSYS and with defining case studies, Also a python code was written to perform this automatic sensitivity calculation by calling HYSYS from python. The main source codes are in Appendix C

6.1 Exhaust gas recirculation (EGR) ratio

To examine the impact of the EGR rate on the NPV, it is necessary to manually adjust the percentage of exhaust gas being recirculated at each step. Throughout each scenario, the amount of recirculated exhaust gas is varied, while several other conditions are held constant: the combustion temperature of the exhaust at 1500 °C, the net electricity output at 400 MW, the minimum approach temperature in the evaporator at (ΔT_{min}) 75 °C, the incoming flue gas temperature entering the absorber is set at 40 °C, the minimum approach temperature in the lean/rich heat exchanger at (ΔT_{min}) 10 °C, and the CO_2 removal efficiency at 90% across adjustments ADJ-1 through ADJ-6. The exhaust gas recirculation rate in the splitter is adjusted in increments of 5%, ranging from 0% to 25%. It is important to note that all other variables and assumptions in this evaluation are kept at their base case default settings.

6.2 Minimum temperature approach in the evaporator (ΔT_{min})

The purpose of this section is to determine the optimal minimum approach temperature (ΔT_{min}) for the evaporator that maximizes the net present value (NPV). NPV can be computed manually in Aspen HYSYS or through a case study that explores various ΔT_{min} values. A specific case study was conducted to assess the economic performance of the lean/rich amine heat exchanger by varying ΔT_{min}.

In this study, ΔT_{min} was adjusted by altering the temperature of outlet steam from evaporator. This adjustment was made during ADJ-3, while other conditions were maintained as follows: the exhaust combustion temperature at 1500°C, net electricity generation at 400 MW, the incoming flue gas temperature to the absorber at 40 °C, the minimum approach temperature in the lean/rich heat exchanger at 10 °C, and CO_2 removal efficiency at 90%, across adjustments ADJ-1 through ADJ-2 and ADJ-4 through ADJ-6.

For the baseline scenario, a minimum approach temperature of 75 °C was initially considered. During this analysis, ΔT_{min} was varied from 25°C to 80°C. Throughout this evaluation, other critical parameters, such as the number of stages in the absorber and the temperature of the flue gas post-pre-cooler, were held constant.

6.3 Minimum temperature approach in the lean/rich heat exchanger (ΔT_{min})

The purpose of this section is to determine the optimal minimum approach temperature (ΔT_{min}) for the lean/rich amine heat exchanger that maximizes the net present value (NPV). NPV can be computed manually in Aspen HYSYS or through a case study that explores various ΔT_{min} values. A specific case study was conducted to assess the economic performance of the lean/rich amine heat exchanger by varying ΔT_{min}.

In this study, ΔT_{min} was adjusted by altering the outlet temperature of the rich amine from the heat exchanger, with the boiler outlet temperature held constant at 120°C. This adjustment was made during ADJ-5, while other conditions were maintained as follows: the exhaust combustion temperature at 1500°C, net electricity generation at 400 MW, the minimum approach temperature in the evaporator at 75 °C, the incoming flue gas temperature to the absorber at 40 °C, and CO_2 removal efficiency at 90%, across adjustments ADJ-1 through ADJ-4 and ADJ-6.

For the baseline scenario, a minimum approach temperature of 10 °C was initially considered. During this analysis, ΔT_{min} was varied from 5°C to 35°C. Throughout this evaluation, other critical parameters, such as the number of stages in the absorber and the temperature of the flue gas post-pre-cooler, were held constant.

7 Results

In this chapter, we will present and discuss the cost estimation outcomes for the base case and the sensitivity analysis of the parameters defined in Chapter 6. Subsequently, we will reveal and explore the results of a modified case that is based on the optimal parameters identified through the sensitivity analysis.

7.1 Base case results

This section delves into the specifics of the CAPEX, OPEX and the revenue generated from the electricity sold by the combined gas power plant. Following this, the payback period is determined using the net present value (NPV) of the project.

7.1.1 CAPEX results

The base case study outlines the equipment costs for the gas-based power plant coupled with the CO_2 capture system, detailed in Table 7.1. The total estimated cost of the equipment amounts to 1516 million euros, with the gas turbine and compressor being the most costly components, accounting for approximately 43% and 42% of the total cost, respectively.

Additional significant costs are associated with the steam turbines, lean/rich amine heat exchangers, absorbers, and evaporators, which contribute 4.8%, 3%, 2.7%, and 1.7% to the total cost, respectively.

Table 7.1: Installed costs of equipment for the gas-based power plant integrated with the CO_2 capture plant.

Equipment	Installed Cost [MEUR]	Relative CAPEX [%]
Gas Turbine	646.31	42.64
Steam Turbine No.1	61.05	4.03
Steam Turbine No.2	11.62	0.77
Compressor	630.52	41.60
Water Pump	2.37	0.16
Evaporators	25.83	1.70
Condenser	6.41	0.42
Separator No.1	1.02	0.07
Separator No.2	6.16	0.41
Absorber (Shell)	20.84	1.37
Absorber (Packing)	20.54	1.36
Desorber (Shell)	3.67	0.24
Desorber (Packing)	2.40	0.16
Lean/rich HEX	45.68	3.01

Lean MEA Cooler	4.65	0.31
Reboiler-D	10.66	0.70
Fan	10.12	0.67
Lean Pump	1.10	0.07
Rich Pump	0.98	0.06
Inlet Cooler	2.83	0.19
Condenser-D	0.89	0.06
Total CAPEX	**1516**	**100**

7.1.2 OPEX results

The annual operational expenses (OPEX) for the base scenario total approximately 106 million euros, as detailed in Table 6.2. Maintenance and natural gas are the principal expenditures for this facility, incurring costs of 60.08 million euros and 26.56 million euros respectively. These represent about 57% and 25% of the total OPEX. Other significant expenses include solvent MEA, electricity for the CO_2 capture plant, and cooling water, which constitute 7.7%, 5.3%, and 4% of the total costs, respectively.

Table 7.2: Operational costs for the CO_2 capture plant integrated with the gas-based power plant

Topic	OPEX [MEUR/Year]	Relative to total OPEX [%]
Electricity	5.65	5.33
Natural gas	26.56	25.03
Cooling water	4.191	3.95
Water process	0.14	0.13
Solvent MEA	8.21	7.74
Operator	0.96	0.90
Engineer	0.31	0.29
Maintenance	60.08	56.63
Total OPEX	**106**	**100**

7.1.3 Revenue and income results

The gas-based power plant generates approximately 400 MW of electricity, operating for 8,000 hours annually. The electricity is sold at a rate of 0.09 euros per kWh, resulting in annual revenue from electricity sales amounting to 287.9 million euros.

Table 7.3 details the electricity generation and consumption specifics for the equipment used in the gas-based power plant.

Table 7.3: Generation and consumption electricity by equipment in the power plant

Equipment	Generation & consumption of electricity [MW]
Gas turbine	596.2
Steam turbine No.1	87.1
Steam turbine No.1	20.72
Compressor	-302.2
Water pump	-1.859
Net output	**400**

7.1.4 Payback period (PBP)

NPV of the base case, covering all the construction and operation durations, is presented in Table 7.4. Construction is expected to span three years, with an operational duration projected at twenty-two years. By the sixteenth year of operation, which corresponds to the eighteenth year in the table, the NPV turns positive, signaling a payback period of sixteen years.

Table 7.4: Net present value during the construction and operation period

Table 7.4: NPV of the project

Year	NPV [MEUR]
0	-505
1	-975
2	-1412
3	-1266
4	-1129
5	-1003
6	-885
7	-775
8	-673
9	-578
10	-490
11	-408
12	-331
13	-260
14	-194

15	-133
16	-76
17	-22
18	27
19	73
20	116
21	155.8
22	192.9
23	227.3
24	259.4
25	289

Additionally, Figure 7.1 demonstrates the project's payback period, showing the net present value (NPV) annually.

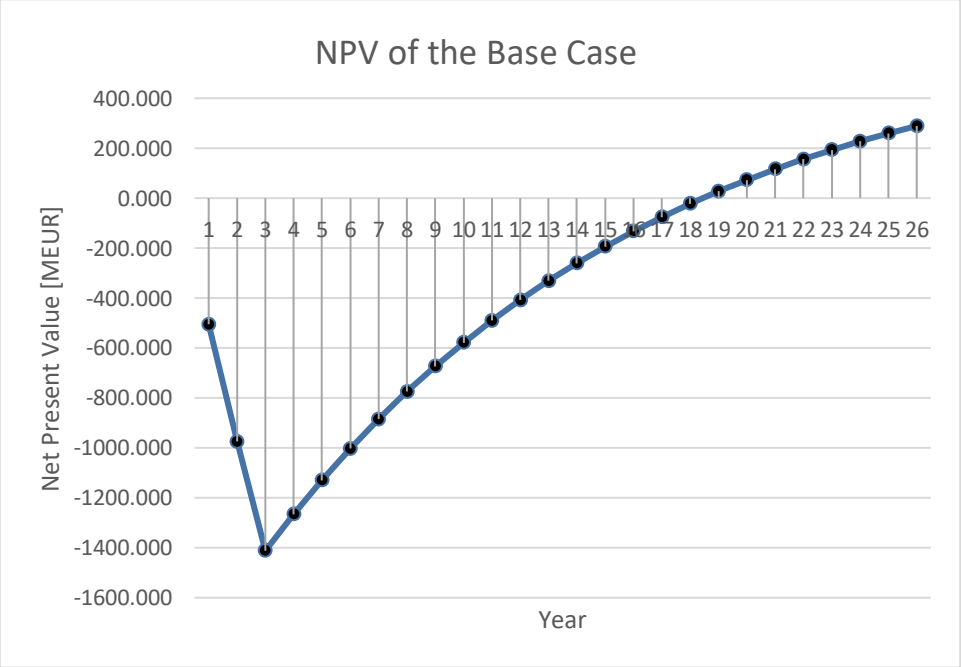

Figure 7.1: NPV and payback period of the base case

7.2 Cost optimization

This section will explore the results from modifying process parameters outlined in the sensitivity analysis in Chapter 6. The approach focuses on cost optimization of these

parameters. For each case study, the optimal parameter chosen is the one that yields the highest NPV for the gas-based power plant combined with the CO_2 capture facility.

7.2.1 Exhaust Gas Recirculation (EGR) ratio

At this step a sensitivity was done on different parameters when we are changing the EGR ratio from 0 to 35 %.Figure 7.2 shows the changes in net present value of the project after 25 years in different EGR ratios. As can be seen in both cases (electricity price of 0.09 euro/kwh and 0.1 euro/kwh), zero EGR ratio has the highest NPV (Figure 3.2).

To evaluate if lowering the compressor price might make EGR more cost-effective than not having EGR, another scenario was defined by reducing the compressor base case unit price to 1.05E5 KEUR from 1.575E5 KEUR (Figure 7.3). However, the results show that decreasing the compressor price did not make EGR more cost-effective than the base case either.

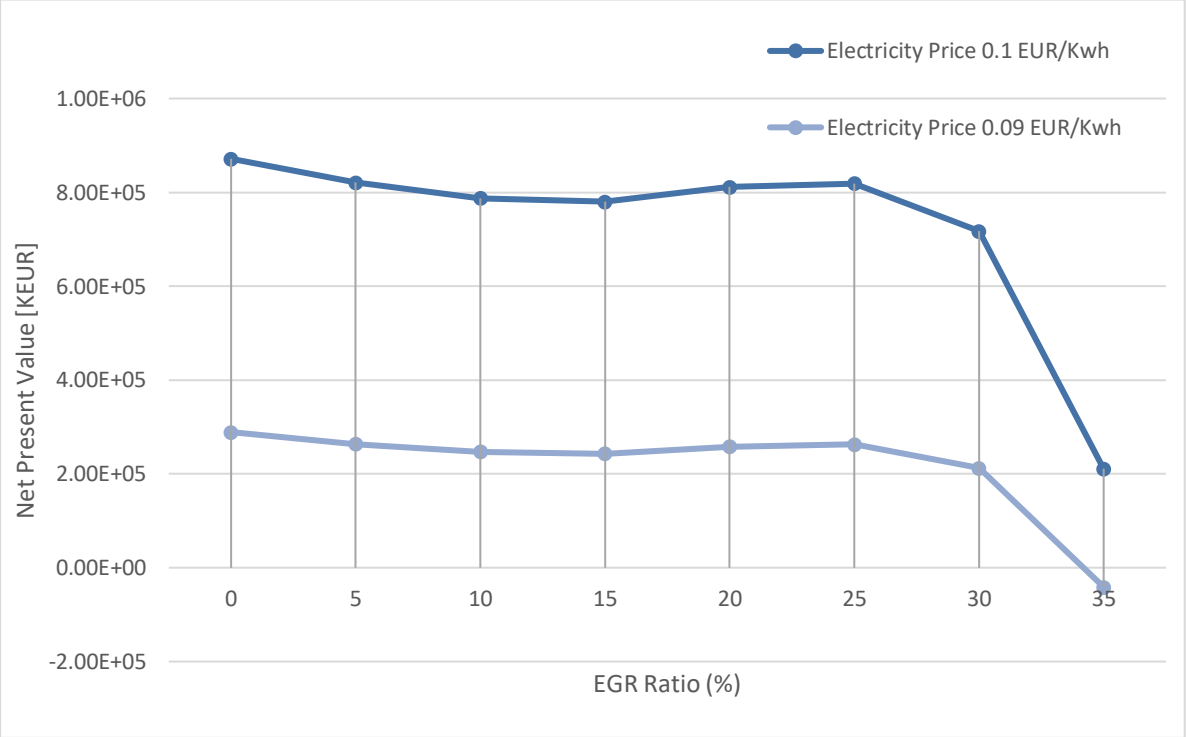

Figure 7.2: Net present value as a function of EGR ratio and electricity price

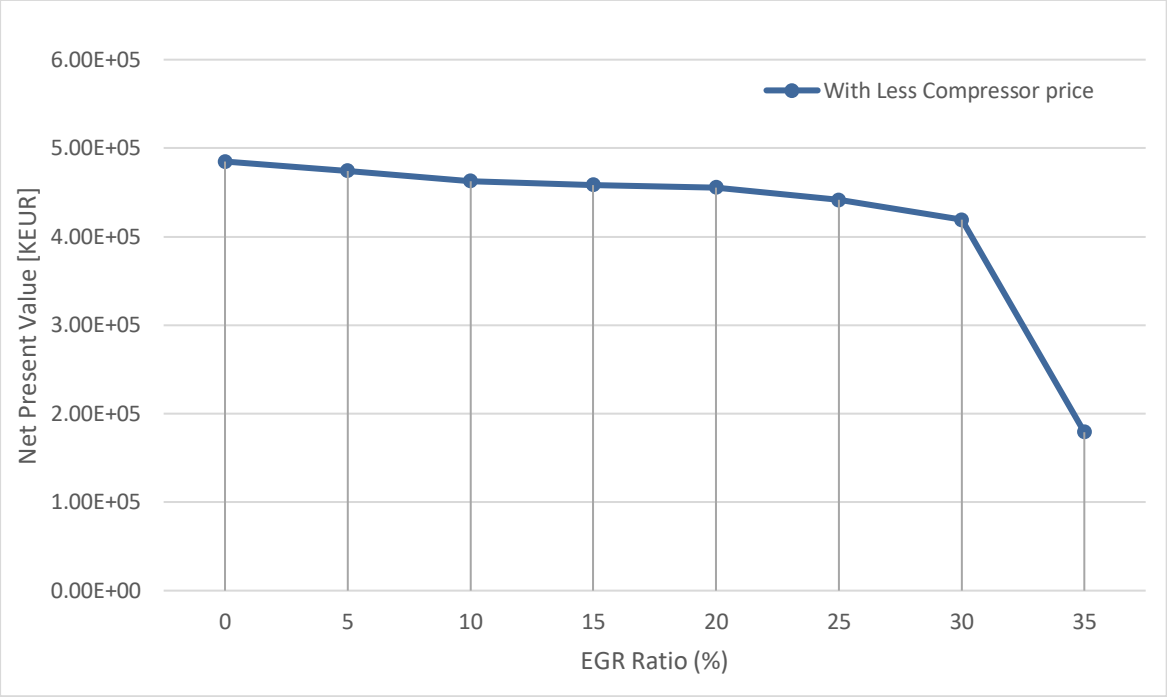

Figure 7.3: Net present value as a function of EGR ratio (with less compressor price)

Besides that Table 7.5 shows the reboiler duty, compressor price, absorber price, exhaust gas flow rate and its CO_2 concentration in different EGR ratios (from 0 to 25 percent). Aso Figures 7.4 to 7.8 demonstrate their respective graphs.

Table 7.5: Changes of some process parameters by altering EGR ratio

EGR ratio	Reboiler duty	Compressor price	Absorber price-	Disrober price-	Gas flow rate to absorber	CO_2 concentration
(Precent)	(KW)	KEURO	KEURO	(KEURO)	Kmol/h	(Mol %)
0	1.65E+05	6.31E+05	4.14E+04	6.07E+03	7.13E+04	4.66
2.5	1.66E+05	6.44E+05	4.10E+04	6.11E+03	7.13E+04	4.67
5	1.66E+05	6.48E+05	4.02E+04	6.08E+03	6.96E+04	4.88
7.5	1.66E+05	6.52E+05	3.93E+04	6.08E+03	6.77E+04	4.92
10	1.66E+05	6.56E+05	3.84E+04	6.09E+03	6.59E+04	5.06
12.5	1.64E+05	6.57E+05	3.71E+04	6.01E+03	6.36E+04	5.22
15	1.61E+05	6.62E+05	3.61E+04	5.84E+03	6.20E+04	5.35
17.5	1.62E+05	6.63E+05	3.51E+04	5.90E+03	5.98E+04	5.55
20	1.62E+05	6.63E+05	3.41E+04	5.90E+03	5.74E+04	5.77
22.5	1.59E+05	6.67E+05	3.30E+04	5.80E+03	5.57E+04	5.93
25	1.59E+05	6.72E+05	3.23E+04	5.76E+03	5.40E+04	6.12

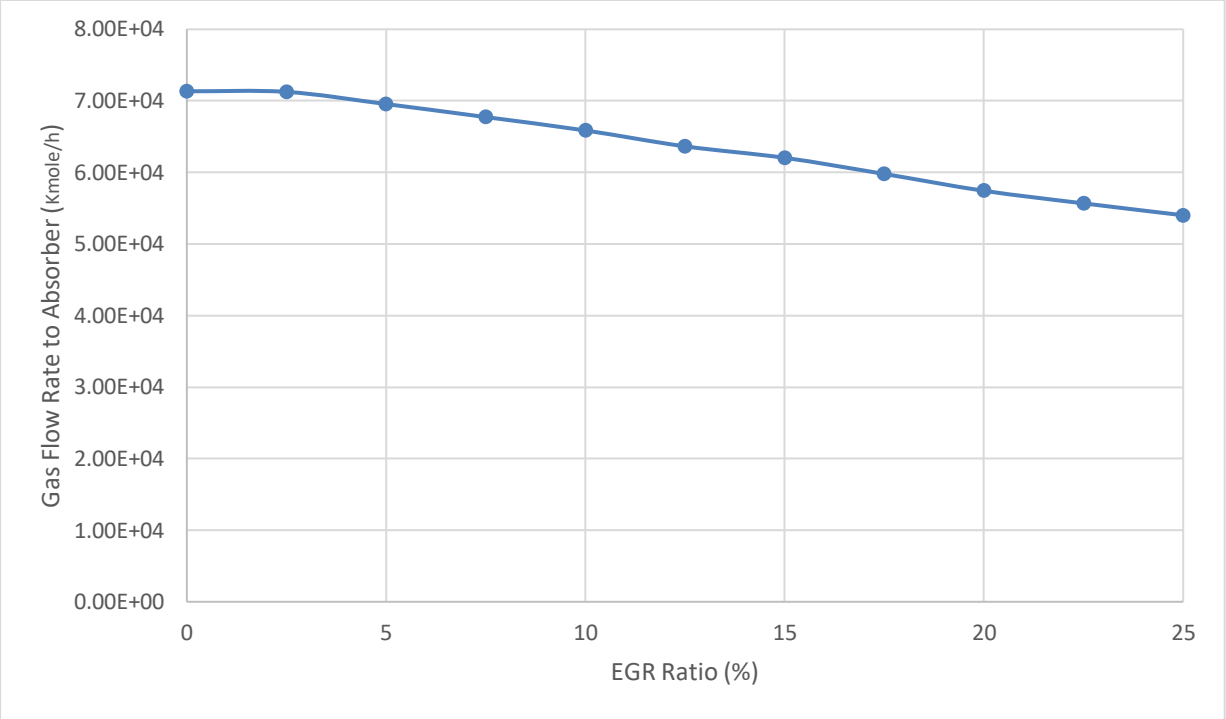

Figure 7.4: The amount of exhaust gas flow rate at different EGR ratios

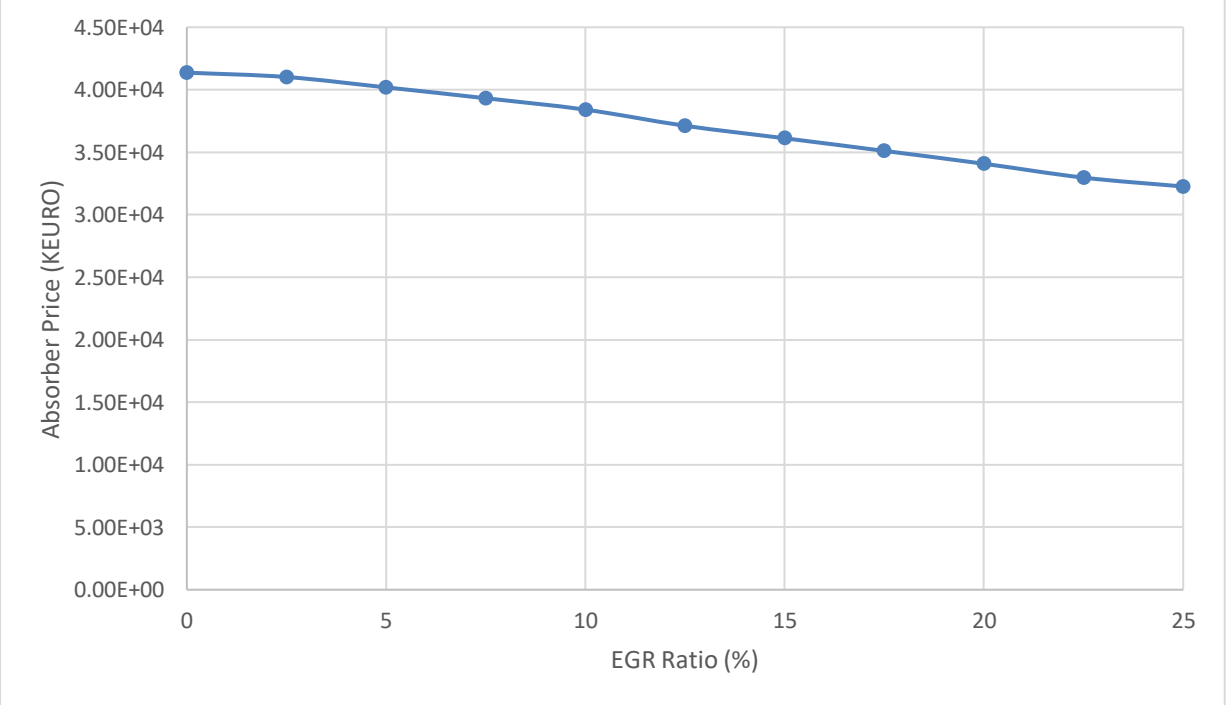

Figure 7.5: Absorber price for different EGR ratios

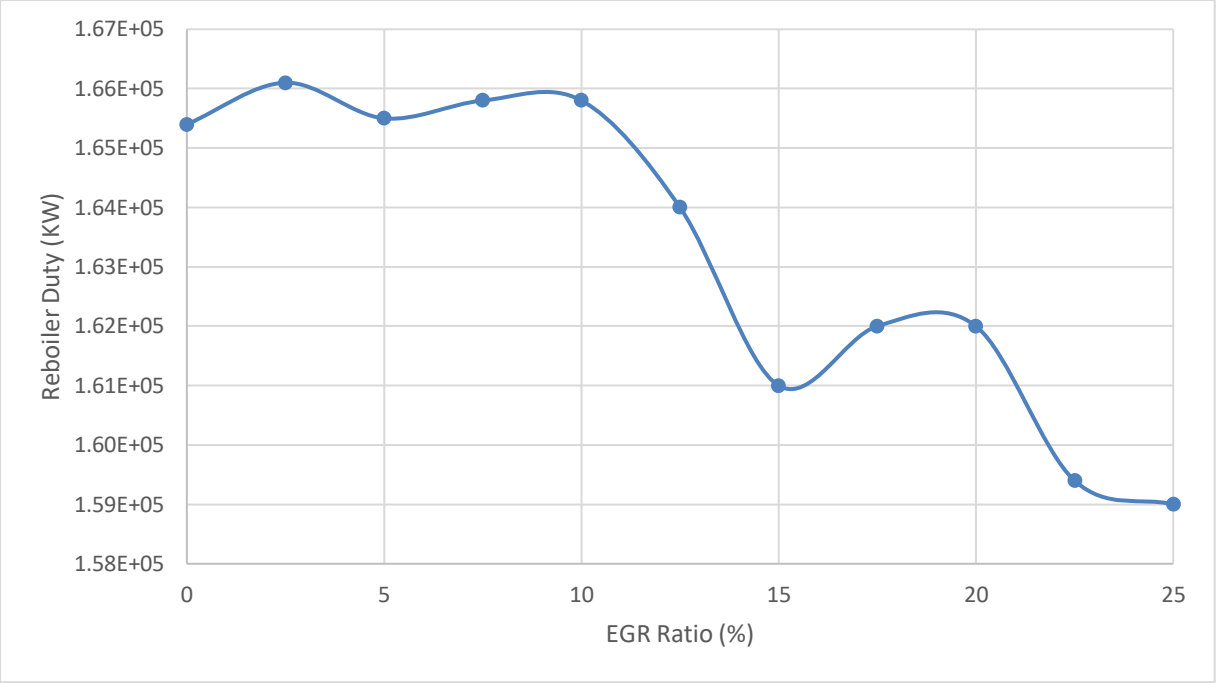

Figure 7.6: Reboiler duty in different EGR ratios

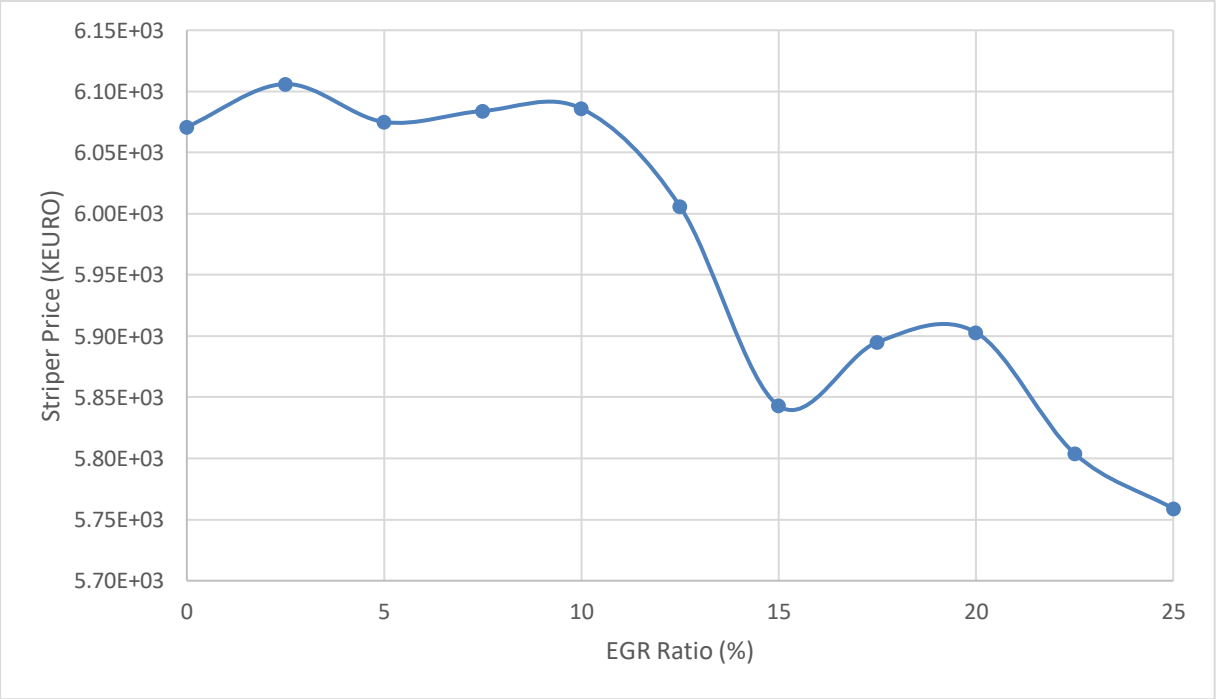

Figure 7.7: Striper (disrober) price for different EGR ratios

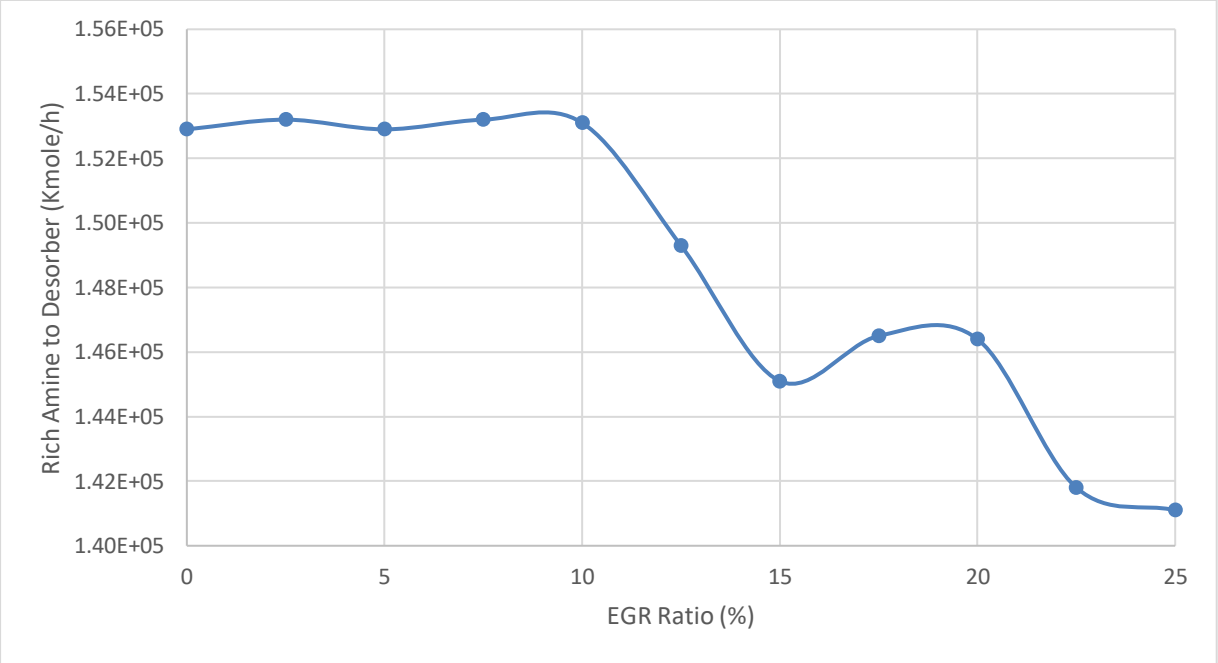

Figure 7.8: Rich amine flow rate of different EGR ratios

7.2.2 Minimum temperature approach (ΔT_{min}) in evaporator

This section aims to optimize the cost by changing the minimum temperature approach (ΔT_{min}) in the evaporator, focusing on achieving the project's highest total NPV. Figure 7.9 and Figure 7.10 show the NPV results when varying the ΔT_{min} from 25 to 85 °C in two different cases for electricity price. The findings indicate that the highest calculated NPV is achieved when the minimum temperature approach is 65 °C and electricity price is 0.09 euro/kwh. When the electricity price increases to 0.1 euro/kwh, the highest NPV is achieved in lower minimum temperature approach (62 °C). Also, the highest NPVs are 2.986E5 MEUR and 6.001E5 MEUR respectively.

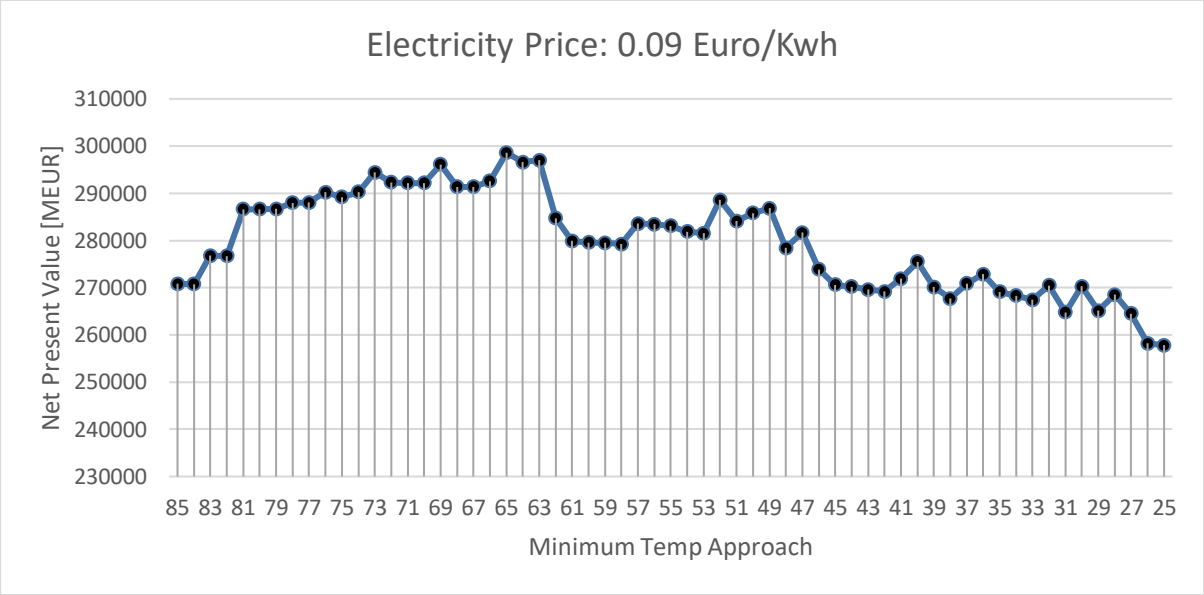

Figure 7.9: NPV as a function of ΔT_{min} in the evaporator (electricity price: 0.09 euro/kwh)

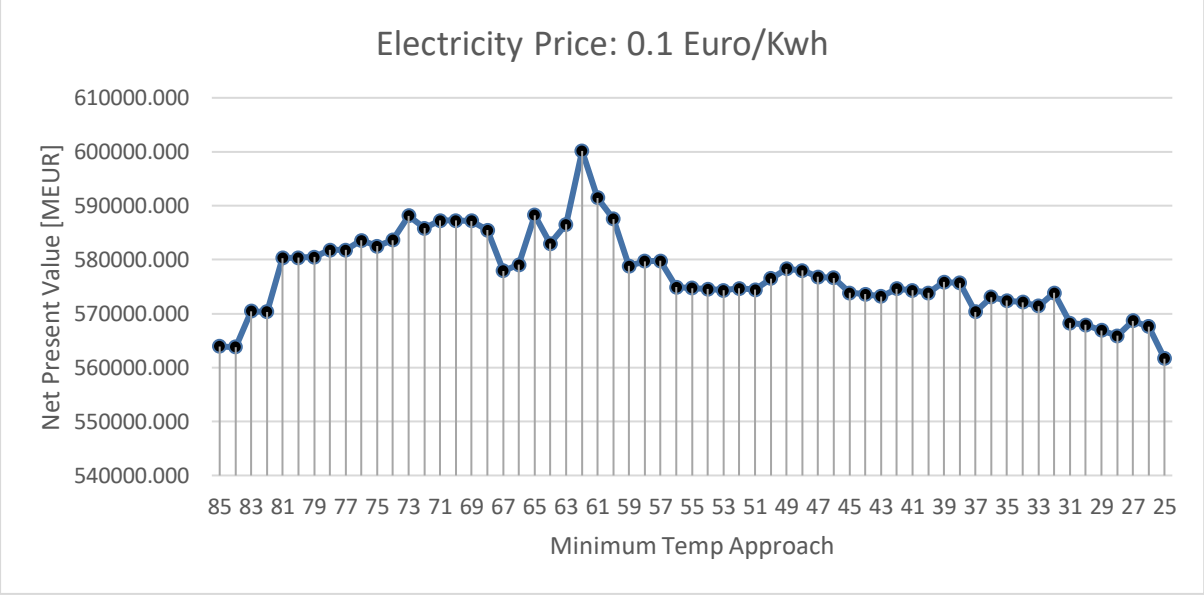

Figure 7.10: NPV as a function of ΔT_{min} in the evaporator (electricity price: 0.1 euro/kwh)

7.2.3 Minimum temperature approach (ΔTmin) in lean/rich heat exchanger

This section aims to optimize ΔT_{min} in the lean/rich heat exchanger, focusing on achieving the project's highest total NPV. Figure 7.11 shows the NPV results when varying the ΔT_{min} from 5 °C to 35 °C. The findings indicate that the highest calculated NPV is achieved when the minimum temperature approach is 20 °C. Also, the highest NPVs is 2.991E5 MEUR.

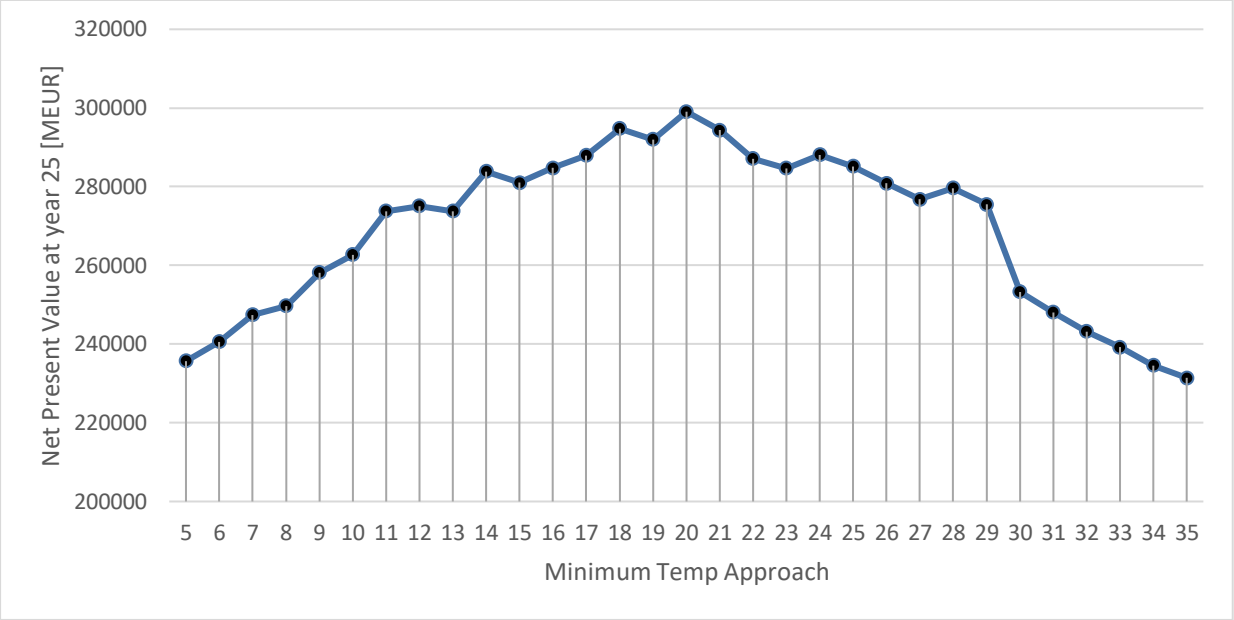

Figure 7.11: NPV as a function of ΔT_{min} in the lean/rich heat exchanger (electricity price: 0.09 euro/kwh)

8 Discussion

In this chanpter, the uncertainty and validity of the attained results will be assessed, followed by a comparison of the results from the previous chapter with formerly similar researchs. Finally, some recommendations for future work will be presented. Addressing these points will undoubtedly enhance future research.

8.1 Evaluation of uncertainty

The uncertainties in the study stem from various factors, including the assumptions used for simulation, dimensioning, cost, and income estimation:

- The goal of cost estimation is to identify the optimal process variables rather than determine the exact absolute values. The potential variations in different configurations contribute to the uncertainty of the assessed costs. The projected overall investment values, covering utility infrastructure, land, and other factors, show significant discrepancies. Evaluating these modifications is not within the scope of this research.
- There are significant uncertainties when estimating the cost of process equipment, especially concerning major equipment installation costs. For high-cost items in the power plant, such as compressors and gas turbines, substantial sources of uncertainty exist. These two items account for 85% of the total CAPEX, totaling 1277 million euros. Given their high cost, greater accuracy and detail are necessary for dimensioning, equipment cost estimation, and the installation factor value in the actual project. Consulting vendors and comparing components in other projects can enhance accuracy.
- The value of electricity, utilized to calculate income from electricity sales, is a major source of uncertainty. While a sensitivity analysis on the effect of electricity price on NPV was conducted, the electricity price was assumed to be fixed for the entire project lifespan, based on the average price in 2023. However, it will undoubtedly fluctuate over the 25-year project duration.
- The project's lifetime was estimated to be 25 years, assuming all equipment would have the same lifespan. In reality, each item's working lifespan will vary. Thus, investigating the lifetime of each piece of equipment individually is necessary for more accurate cost calculations.
- When selecting equipment types in the dimensioning phase, only basic and essential factors were considered. Including additional factors in the equipment design would provide more precise options, thereby improving accuracy. The Aspen Icarus reference guide [47] can be useful for this purpose.
- A more reasonable equipment cost could be obtained by using cost estimation software such as Aspen In-Plan Cost Estimator. However, the accuracy of cost estimation depends

on the number of input factors used. This study considered the minimum necessary input factors, but adding optional inputs can improve accuracy.

- Additional source of uncertainty is the validity of scale-up factors within the indicated range and the used installation factor. The adjustment constant for equipment was 0.65 (but 1.1 for desorber and absorber) also the installation factor for all equipment remained fixed throughout sensitivity analysis, adding uncertainty to cost scaling and affecting the comparison of several process parameters.
- Natural gas price and maintenance cost are major sources of uncertainty between operating costs. The maintenance fee was assumed to be 4% of the total CAPEX, accounting for about 57% of the operating cost. The natural gas price was assumed to be constant throughout the project's lifespan, but it is expected to fluctuate, impacting the total cost estimate. For greater precision, considering different utility prices and annual cost changes is recommended.
- The assumptions and specifications selected may affect the calculated cost and optimal values. For example, the type of packing affects the height and cost of the desorption and absorption columns. The ΔT_{min} calculations depend on various factors, like the overall heat transfer coefficient of the lean/rich heat exchanger.
- This study estimated costs considering only the major pieces of equipment in the power plant as well as the capture plant. Including more items would enhance the accuracy and precision of the estimation.
- A constant Murphree efficiency simplification in desorber's and absorber may impact the calculations, potentially leading to errors in the amine circulation flow and, consequently, the estimated plant cost.
- Other uncertainties in the simulation results likely relate to sensitivity analysis and defining tolerances for each adjustment block. The model includes six adjustment blocks, each requiring convergence after each sensitivity analysis. Each block has an accepted tolerance deviation (error) from its target value, introducing uncertainty and fluctuation into the results.

8.2 Comparison of with earlier studies

This project reports the base case cost estimation as well as cost optimization of the some of the primary parameters in a gas-based power plant which is integrated with the amine-based CO_2 capture. Lots of earlier investigates have only the cost optimization of a CO_2 capture plant into the consideration. However, only Aboukazempour Amiri [32] simultaneously considered the cost optimization of a gas-based power plant combined with an amine-based CO_2 capture plant [32], although most of the parameters he analyzed differed from those examined in this research. Nevertheless, some usual parameters in the cost optimization of the CO_2 capture section can be utilized for comparison among the parameters used in the sensitivity analysis.

Regarding the gas-based power plant segment, there are few sources providing data on the relevant parameters considered, and it must be mentioned that these information are not based on the cost optimization approach.

The results of simulating the base case setup for the current project in the CO_2 capture plant part are compared with previous studies outcome in this field through Table 8.1.

Table 8.1: Analogy of the base case specification with prior studies in the CO_2 capture plant part

Authors/Date	Ref.	CO_2 Rem. Eff [%]	ΔTmin in Lean/rich HEX [°C]	CO_2 Concen. (mole %)	No. of Absorber stages
Øi et al./ 2007	[15]	85	10	3.75	10
Kallevik /2010	[46]	85	14	5.9	15
Sipöcz et al./ 2011	[56]	90	10	4.2	NA
Amrollahi et al./ 2011	[55]	90	8.5	3.8	13
Ricardez-Sandoval /2016	[57]	90	-	4.3	25
Nwaoha et al./ 2018	[58]	90	10	11.5	36
Ali et al./ 2019	[51]	90	10	22 - 28	15
Aromada et al./ 2021	[41]	85	10	3.73	20
Øi et al./ 2021	[45]	90	10	17.8	12
Shirdel et al./2022	[59]	90	10	7.5	20
Aboukazempour Amiri/2023	[32]	85	10	5.39	10
Current project/2024	-	90	20	4.66	10

8.2.1 Exhaust Gas Recirculation (EGR) ratio

The results of varying the EGR ratio from 0% to 35% indicated that the most cost-effective scenario in this project is a zero EGR ratio and the highest NPV (equal to 289 MEUR) is achieved at zero EGR (Figure 7.2). Increasing the EGR ratio presents a trade-off: the compressor cost rises with a higher EGR ratio (Table 7.5), while the size and cost of the absorber and desorber decrease due to the inverse relationship between exhaust gas flow rate and EGR ratio (Figure 7.5 and Figure 7.7). Additionally, Figure 7.6 shows that reboiler duty decreases as the rich amine flow rate reduces. However, the increase in compressor cost with a higher EGR ratio outweighs the total reduction in absorber, desorber, and reboiler duty costs. Therefore, the optimal NPV is found at zero EGR. Even increasing electricity prices, which would amplify the effect of reboiler duty in the sensitivity analysis, does not make a higher

EGR ratio more cost-efficient than a zero EGR ratio (Figure 7.2). Similarly, Figure 7.3 demonstrates that reducing the base cost of the compressor, slightly alters the slope of NPV reduction with increasing EGR ratio, but the optimal scenario remains at zero EGR.

Comparing these results with other research shows that Sipöcz and Tobiesen [20] and Luo et al. [21] obtained similar findings, indicating that EGR reduces the size of the absorber and desorber as well as the reboiler duty. But in ther other hand, Sipöcz and Tobiesen [20] found EGR ratio higher than 0 (40%) as the optimum scenario. That might be explained by their different cost estimation method and their CAPEX and OPEX assumptions. Also, it is a possibility that they found a really favorable alternative.

8.2.2 Minimum temperature approach in the evaporator

Based on the result of optimization of ΔT_{min} in the current project, for the electricity price of 0.09 Euro/kwh the highest NPV achieved at minimum temperature approach of 66 °C. But by increasing the energy price to 0.1 Euro/kwh the minimum temperature approach decreased to 62 °C. The reason behind that can be because by increasing the electricity price, the energy gets higher value and to get higher NPV we should save more energy, the optimum minimum temperature approach would decrease.

8.2.3 Minimum temperature approach in the lean/rich heat exchanger

Based on the cost optimization results for ΔT_{min} in this study, a temperature difference of 20 °C yields the highest net present value. In contrast, Aboukazempour Amiri's project identified an optimal ΔT_{min} of around 13 °C [60].Also, corresponding to Øi et al. [45], the optimal minimum temperature approach usually ranges from 10 °C to 15 °C, depending on specific circumstances. Most relevant evaluations have specifically noted 13 °C as the ideal scenario [15], [45], [50], [59], [61].

Reducing ΔT_{min} minimizes energy consumption in the reboiler, leading to lower steam demand and higher electricity generation in the steam turbines, thereby increasing the net present value. However, a lower ΔT_{min} also requires a larger heat exchanger surface area, raising capital costs and reducing net present value. The optimal ΔT_{min} is determined by balancing these cost factors. The difference between the results of Aboukazempour Amiri's work [32] and this study may be attributed to the varying electricity prices in the two cases (0.134 Euro/KWh in Aboukazempour Amiri's work [32]).[26]

8.3 Proposition for upcoming work

Here are some recommendations for further research in the current field to improve the reliability and accuracy of simulation and cost optimization:

- Include carbon emission penalties and carbon prices to optimize the techno economical assessment.
- Optimize the cost of absorption column stages by adjusting Murphree efficiency.
- Optimize combustion exhaust temperature (turbine inlet temperatures) in sensitivity analysis for optimal cost-effectiveness.
- Consider CO_2 transport and storage when executing simulations and cost estimations.
- Increase steam cycle pressure levels from two to three (HP, IP, and LP) to optimize steam usage and power generation efficiency.
- Incorporate the Murphree efficiency relationship in the inlet flue gas temperature cost optimization. Adjusting the Murphree efficiency for different inlet flue gas temperatures can improve the absorber column's temperature profile and analysis performance.
- Account for potential changes in electricity and fuel prices over the project's duration.
- Using Python to conduct sensitivity analysis in Aspen HYSYS, and integrating it with other software (such as Aspen In-Plant) and Excel worksheets, allows for performing extensive sensitivity analysis. This approach helps in finding the optimal parameters by creating a matrix of NPVs from various scenarios.

9 Conclusion

This study centers on the process simulation and cost optimization of amine based CO2 capture integrated with a natural gas based power plant using Aspen HYSYS. The entered information for the gas-based power plant model is obtained from prior research.

The model simulation comprises two main sections: a natural gas-based power plant and a CO_2 capture plant. The flue gas produced by the power plant, following power production in the gas turbines and heat transfer in the evaporators, is directly transferred to the capture plant for CO_2 removal. To meet the simulation requirements and facilitate the design of an automated simulation model, six adjustment operations have been incorporated. The combustion temperature is regulated by the air input flow rate using ADJ-1, set to 1500 °C. The net electricity output is determined by the natural gas flow rate with ADJ-2, set to 400 kW. The minimum temperature approach in the evaporator is controlled by ADJ-3, with a target value of 75 °C. ADJ-4 adjusts the cooling water requirement in the inlet cooler to achieve a flue gas temperature of 40 °C at the absorber. The minimum temperature approach in the lean/rich heat exchanger (10 °C) is controlled by the rich amine outlet temperature using ADJ-5. Finally, the CO_2 removal efficiency, set to 90%, is adjusted by changing the lean amine flow rate using ADJ-6.

To enhance the simulation's efficiency, three additional recycling blocks have been implemented. The first one is used for exhaust gas recycling process. RCY-2 is used for the water recycling process in the steam turbine, and RCY-3 is lean amine recirculation process line.

The NPV of the base case simulation is estimated using CAPEX, OPEX, and revenue from selling power. Capital costs were determined using the Aspen In-Plant Cost Estimator and EDF based on the main equipment dimensions. The NPV method served as the criterion for evaluating the overall cost of the simulation. The simulation results of the base case indicate a NPV of 289 million euros in the project lifespan (25 years) and the payback period of 16 years.

Cost optimization was conducted using sensitivity analysis to minimize expenses. When equipment sizes were adjusted through sensitivity analysis and the equipment costs were modified via the Power-Law. The sensitivity analysis focused on the EGR ratio, minimum temperature approach in the lean/rich heat exchanger, and minimum temperature approach in the evaporator to achieve the highest net present value for the project.

The results reveal that the highest NPV is obtained with a zero EGR rate. In the power plant the compressor size would increase with higher EGR rates as the gas flow rate to compressor rises. Additionally, increasing the EGR rate leads to a larger compressor size and smaller absorber, reboiler size and less reboiler duty. Also, the exhaust gas flow rate decreases, and

CO_2 concentration in the exhaust gas increases. These details result from the CO_2 capture part, are all in consistency with previous studies.

The sensitivity analysis for calculating ΔT_{min} in the lean/rich heat exchanger involves balancing the cost between external utility consumption and the heat exchanger area. Reducing ΔT_{min} lowers the energy consumption of the reboiler, which in turn decreases the steam demand and allows for increased electricity production in the steam turbines, thereby increasing the net present value. Cost optimization of ΔT_{min} indicates that a value of 20 °C yields the highest net present value.

For the evaporator, the cost trade-off was between the evaporator area and the amount of energy produced in the steam turbines. Increasing the minimum temperature approach reduces the evaporator size and cost, but it also lowers the steam temperature supplied to the steam turbines, which decreases electricity production. Conversely, decreasing the minimum temperature approach increases both the evaporator cost and electricity production. The optimal ΔT_{min}, which provides the highest NPV, is achieved with a minimum temperature approach of 65 °C at an electricity price of 0.09 Euro/KWh and 62 °C at an electricity price of 0.10 Euro/KWh.

References

[1] V. Z. Castillo, H.-S. D. Boer, R. M. Muñoz, D. E. H. J. Gernaat, R. Benders, and D. Van Vuuren, "Future global electricity demand load curves," *Energy*, vol. 258, p. 124741, Nov. 2022, doi: 10.1016/j.energy.2022.124741.

[2] "Share of energy consumption by source," Our World in Data. Accessed: Nov. 03, 2023. [Online]. Available: https://ourworldindata.org/grapher/share-energy-source-sub

[3] V. Ş. Ediger, "An integrated review and analysis of multi-energy transition from fossil fuels to renewables," *Energy Procedia*, vol. 156, pp. 2–6, Jan. 2019, doi: 10.1016/j.egypro.2018.11.073.

[4] A. Kalair, N. Abas, M. S. Saleem, A. R. Kalair, and N. Khan, "Role of energy storage systems in energy transition from fossil fuels to renewables," *Energy Storage*, vol. 3, no. 1, p. e135, Feb. 2021, doi: 10.1002/est2.135.

[5] R. York and S. E. Bell, "Energy transitions or additions?," *Energy Res. Soc. Sci.*, vol. 51, pp. 40–43, May 2019, doi: 10.1016/j.erss.2019.01.008.

[6] "IEA – International Energy Agency." [Online]. Available: https://www.iea.org

[7] "Natural Gas Combined Cycle - an overview." [Online]. Available: https://www.sciencedirect.com/topics/engineering/natural-gas-combined-cycle

[8] E. Rubin, A. Rao, and C. Chen, "Comparative assessments of fossil fuel power plants with CO_2 capture and storage," in *Greenhouse Gas Control Technologies 7*, vol. I, Elsevier, 2005, pp. 285–293. doi: 10.1016/B978-008044704-9/50029-X.

[9] M. H. W. N. Jinadasa, K.-J. Jens, and M. Halstensen, "Process Analytical Technology for CO_2 Capture," in *Carbon Dioxide Chemistry, Capture and Oil Recovery*, I. Karamé, J. Shaya, and H. Srour, Eds., InTech, 2018. doi: 10.5772/intechopen.76176.

[10] C. Song, Q. Liu, S. Deng, H. Li, and Y. Kitamura, "Cryogenic-based CO_2 capture technologies: State-of-the-art developments and current challenges," *Renew. Sustain. Energy Rev.*, vol. 101, pp. 265–278, 2019.

[11] H. A. Patel, J. Byun, and C. T. Yavuz, "Carbon Dioxide Capture Adsorbents: Chemistry and Methods," *ChemSusChem*, vol. 10, no. 7, pp. 1303–1317, Apr. 2017, doi: 10.1002/cssc.201601545.

[12] J. Singh and D. W. Dhar, "Overview of Carbon Capture Technology: Microalgal Biorefinery Concept and State-of-the-Art," *Front. Mar. Sci.*, vol. 6, p. 29, Feb. 2019, doi: 10.3389/fmars.2019.00029.

[13] M. K. Lam, K. T. Lee, and A. R. Mohamed, "Current status and challenges on microalgae-based carbon capture," *Int. J. Greenh. Gas Control*, vol. 10, pp. 456–469, Sep. 2012, doi: 10.1016/j.ijggc.2012.07.010.

[14] A. I. Osman, M. Hefny, M. I. A. Abdel Maksoud, A. M. Elgarahy, and D. W. Rooney, "Recent advances in carbon capture storage and utilisation technologies: a review," *Environ. Chem. Lett.*, vol. 19, no. 2, pp. 797–849, Apr. 2021, doi: 10.1007/s10311-020-01133-3.

[15] L. E. Øi, "Aspen HYSYS Simulation of CO 2 Removal by Amine Absorption from a Gas Based Power Plant," presented at the SIMS2007 Conference, Gøteborg, Oct. 2007.

[16] A. Mathisen, G. Hegerland, N. H. Eldrup, R. Skagestad, and H. A. Haugen, "Combining bioenergy and CO_2 capture from gas fired power plant," *Energy Procedia*, vol. 4, pp. 2918–2925, 2011, doi: 10.1016/j.egypro.2011.02.199.

[17] H. Li, G. Haugen, M. Ditaranto, D. Berstad, and K. Jordal, “Impacts of exhaust gas recirculation (EGR) on the natural gas combined cycle integrated with chemical absorption CO_2 capture technology,” *Energy Procedia*, vol. 4, pp. 1411–1418, 2011, doi: 10.1016/j.egypro.2011.02.006.

[18] L. E. Øi, “Removal of CO_2 from exhaust gas,” Doctoral thesis, Telemark University College, 2012. [Online]. Available: http://hdl.handle.net/11250/2437805

[19] M. Karimi, M. Hillestad, and H. F. Svendsen, “Natural Gas Combined Cycle Power Plant Integrated to Capture Plant,” *Energy Fuels*, vol. 26, no. 3, pp. 1805–1813, Mar. 2012, doi: 10.1021/ef201921s.

[20] N. Sipöcz and F. A. Tobiesen, “Natural gas combined cycle power plants with CO_2 capture – Opportunities to reduce cost,” *Int. J. Greenh. Gas Control*, vol. 7, pp. 98–106, Mar. 2012, doi: 10.1016/j.ijggc.2012.01.003.

[21] X. Luo, M. Wang, and J. Chen, “Heat integration of natural gas combined cycle power plant integrated with post-combustion CO_2 capture and compression,” *Fuel*, vol. 151, pp. 110–117, Jul. 2015, doi: 10.1016/j.fuel.2015.01.030.

[22] X. Luo and M. Wang, “Optimal operation of MEA-based post-combustion carbon capture for natural gas combined cycle power plants under different market conditions,” *Int. J. Greenh. Gas Control*, vol. 48, pp. 312–320, May 2016, doi: 10.1016/j.ijggc.2015.11.014.

[23] A. Alhajaj, N. Mac Dowell, and N. Shah, “A techno-economic analysis of post-combustion CO 2 capture and compression applied to a combined cycle gas turbine: Part I. A parametric study of the key technical performance indicators,” *Int. J. Greenh. Gas Control*, vol. 44, pp. 26–41, Jan. 2016, doi: 10.1016/j.ijggc.2015.10.022.

[24] A. Alhajaj, N. Mac Dowell, and N. Shah, “A techno-economic analysis of post-combustion CO 2 capture and compression applied to a combined cycle gas turbine: Part II. Identifying the cost-optimal control and design variables,” *Int. J. Greenh. Gas Control*, vol. 52, pp. 331–343, Sep. 2016, doi: 10.1016/j.ijggc.2016.07.008.

[25] A. Alhajaj, N. Mac Dowell, and N. Shah, “A techno-economic analysis of post-combustion CO 2 capture and compression applied to a combined cycle gas turbine: Part II. Identifying the cost-optimal control and design variables,” *Int. J. Greenh. Gas Control*, vol. 52, pp. 331–343, Sep. 2016, doi: 10.1016/j.ijggc.2016.07.008.

[26] Y. Hu, G. Xu, C. Xu, and Y. Yang, “Thermodynamic analysis and techno-economic evaluation of an integrated natural gas combined cycle (NGCC) power plant with post-combustion CO_2 capture,” *Appl. Therm. Eng.*, vol. 111, pp. 308–316, Jan. 2017, doi: 10.1016/j.applthermaleng.2016.09.094.

[27] R. Dutta, L. O. Nord, and O. Bolland, “Selection and design of post-combustion CO_2 capture process for 600 MW natural gas fueled thermal power plant based on operability,” *Energy*, vol. 121, pp. 643–656, Feb. 2017, doi: 10.1016/j.energy.2017.01.053.

[28] Y. Hu, Y. Gao, H. Lv, G. Xu, and S. Dong, “A New Integration System for Natural Gas Combined Cycle Power Plants with CO_2 Capture and Heat Supply,” *Energies*, vol. 11, no. 11, p. 3055, Nov. 2018, doi: 10.3390/en11113055.

[29] B. Alexanda Petrovic and S. Masoudi Soltani, “Optimization of Post Combustion CO_2 Capture from a Combined-Cycle Gas Turbine Power Plant via Taguchi Design of Experiment,” *Processes*, vol. 7, no. 6, p. 364, Jun. 2019, doi: 10.3390/pr7060364.

[30] M. Gatti *et al.*, “Preliminary Performance and Cost Evaluation of Four Alternative Technologies for Post-Combustion CO_2 Capture in Natural Gas-Fired Power Plants,” *Energies*, vol. 13, no. 3, p. 543, Jan. 2020, doi: 10.3390/en13030543.

[31] A. Ayyad, A. Abbas, and N. Elminshawy, “A simulation study of the effect of post-combustion amine-based carbon-capturing integrated with solar thermal collectors for combined cycle gas power plant,” *Discov. Sustain.*, vol. 2, no. 1, p. 9, Dec. 2021, doi: 10.1007/s43621-021-00018-x.

[32] E. Aboukazempour Amiri, “Process simulation and cost optimization of gas-based power plant integrated with amine-based CO_2 capture,” Master Thesis, University of South-Eastern Norway, Porsgrunn, 2023. [Online]. Available: https://openarchive.usn.no/usn-xmlui/handle/11250/3062462

[33] M. M. Islam, M. Hasanuzzaman, A. K. Pandey, and N. A. Rahim, “Modern energy conversion technologies,” in *Energy for Sustainable Development*, Elsevier, 2020, pp. 19–39. doi: 10.1016/B978-0-12-814645-3.00002-X.

[34] R. Bahrampoury, “Exergetic Optimization of Designing Parameters for Heat Recovery Steam Generators Through Direct Search Method,” *J. Mech. Res. Appl.*, [Online]. Available: https://journals.iau.ir/article_512600.html

[35] A. D. Rao, *Combined cycle systems for near-zero emission power generation*. Woodhead Publishing Limited, 2012. doi: 10.1533/9780857096180.

[36] E. K. Vakkilainen, “Principles of Steam Generation,” in *Steam Generation from Biomass*, Elsevier, 2017, pp. 1–17. doi: 10.1016/B978-0-12-804389-9.00001-0.

[37] C. Song, Q. Liu, S. Deng, H. Li, and Y. Kitamura, “Cryogenic-based CO_2 capture technologies: State-of-the-art developments and current challenges,” *Renew. Sustain. Energy Rev.*, vol. 101, pp. 265–278, Mar. 2019, doi: 10.1016/j.rser.2018.11.018.

[38] S. Orangi, “Simulation and cost estimation of CO_2 capture processes using different solvents/blends,” Master thesis, University of South-Eastern Norway, 2021. [Online]. Available: https://hdl.handle.net/11250/2774682

[39] C. Botero, M. Finkenrath, M. Bartlett, R. Chu, G. Choi, and D. Chinn, “Redesign, Optimization, and Economic Evaluation of a Natural Gas Combined Cycle with the Best Integrated Technology CO_2 Capture,” *Energy Procedia*, vol. 1, no. 1, pp. 3835–3842, Feb. 2009, doi: 10.1016/j.egypro.2009.02.185.

[40] P. A. M. Ystad, “Power Plant with CO_2 Capture based on Absorption: Integration Study,” NTNU, 2010. [Online]. Available: http://hdl.handle.net/11250/234101

[41] S. A. Aromada, N. H. Eldrup, and L. Erik Øi, “Capital cost estimation of CO_2 capture plant using Enhanced Detailed Factor (EDF) method: Installation factors and plant construction characteristic factors,” *Int. J. Greenh. Gas Control*, vol. 110, p. 103394, Sep. 2021, doi: 10.1016/j.ijggc.2021.103394.

[42] S. Fagerheim, “Process simulation of CO_2 absorption at TCM Mongstad,” Master Thesis, University of South-Eastern Norway, 2019. [Online]. Available: https://hdl.handle.net/11250/2644680

[43] S. Laribi, L. Dubois, G. De Weireld, and D. Thomas, “Study of the post-combustion CO_2 capture process by absorption-regeneration using amine solvents applied to cement plant flue gases with high CO_2 contents,” *Int. J. Greenh. Gas Control*, vol. 90, p. 102799, Nov. 2019, doi: 10.1016/j.ijggc.2019.102799.

[44] S. Aforkoghene Aromada and L. Øi, “Simulation of improved absorption configurations for CO_2 capture,” presented at the The 56th Conference on Simulation and Modelling (SIMS 56), October, 7-9, 2015, Linköping University, Sweden, Nov. 2015, pp. 21–29. doi: 10.3384/ecp1511921.

[45] L. E. Øi, N. Eldrup, S. Aromada, A. Haukås, J. HelvigIda Hæstad, and A. M. Lande, “Process Simulation, Cost Estimation and Optimization of CO_2 Capture using Aspen

HYSYS," presented at the SIMS Conference on Simulation and Modelling SIMS 2020, September 22-24, Virtual Conference, Finland, Mar. 2021, pp. 326–331. doi: 10.3384/ecp20176326.

[46] O. B. Kallevik, "Cost estimation of CO_2 removal in HYSYS," Master thesis, Høgskolen i Telemark, 2010. [Online]. Available: http://hdl.handle.net/11250/2439023

[47] "Aspen Icarus Reference Guide." [Online]. Available: https://esupport.aspentech.com/S_Article?id=000098074

[48] R. Sinnott and G. Towler, *Chemical Engineering Design*. 2009. [Online]. Available: https://shop.elsevier.com/books/chemical-engineering-design/sinnott/978-0-7506-8551-1

[49] K. Park and L. E. Øi, "Optimization of gas velocity and pressure drop in CO_2 absorption column," presented at the The 58th Conference on Simulation and Modelling (SIMS 58) Reykjavik, Iceland, September 25th – 27th, 2017, Sep. 2017, pp. 292–297. doi: 10.3384/ecp17138292.

[50] S. A. Aromada, N. H. Eldrup, and L. E. Øi, "Cost and Emissions Reduction in CO_2 Capture Plant Dependent on Heat Exchanger Type and Different Process Configurations: Optimum Temperature Approach Analysis," *Energies*, vol. 15, no. 2, p. 425, Jan. 2022, doi: 10.3390/en15020425.

[51] H. Ali, N. H. Eldrup, F. Normann, R. Skagestad, and L. E. Øi, "Cost Estimation of CO_2 Absorption Plants for CO_2 Mitigation – Method and Assumptions," *Int. J. Greenh. Gas Control*, vol. 88, pp. 10–23, Sep. 2019, doi: 10.1016/j.ijggc.2019.05.028.

[52] R. Smith, *Chemical process design and integration*. Chichester, West Sussex, England ; Hoboken, NJ: Wiley, 2005.

[53] "Average monthly electricity wholesale price in the Nordic countries from January 2019 to March 2024," Statista. [Online]. Available: https://www.statista.com/statistics/1271469/norway-monthly-wholesale-electricity-price/

[54] N. Sipöcz, A. Tobiesen, and M. Assadi, "Integrated modelling and simulation of a 400 MW NGCC power plant with CO_2 capture," *Energy Procedia*, vol. 4, pp. 1941–1948, 2011, doi: 10.1016/j.egypro.2011.02.074.

[55] Z. Amrollahi, P. A. M. Ystad, I. S. Ertesvåg, and O. Bolland, "Optimized process configurations of post-combustion CO_2 capture for natural-gas-fired power plant – Power plant efficiency analysis," *Int. J. Greenh. Gas Control*, vol. 8, pp. 1–11, May 2012, doi: 10.1016/j.ijggc.2012.01.005.

[56] Z. He and L. A. Ricardez-Sandoval, "Dynamic modelling of a commercial-scale CO_2 capture plant integrated with a natural gas combined cycle (NGCC) power plant," *Int. J. Greenh. Gas Control*, vol. 55, pp. 23–35, Dec. 2016, doi: 10.1016/j.ijggc.2016.11.001.

[57] C. Nwaoha, M. Beaulieu, P. Tontiwachwuthikul, and M. D. Gibson, "Techno-economic analysis of CO_2 capture from a 1.2 million MTPA cement plant using AMP-PZ-MEA blend," *Int. J. Greenh. Gas Control*, vol. 78, pp. 400–412, Nov. 2018, doi: 10.1016/j.ijggc.2018.07.015.

[58] S. Shirdel *et al.*, "Sensitivity Analysis and Cost Estimation of a CO_2 Capture Plant in Aspen HYSYS," *ChemEngineering*, vol. 6, no. 2, p. 28, Apr. 2022, doi: 10.3390/chemengineering6020028.

[59] N. Farouk and L. Sheng, "Effect of Ambient Temperature on the Performance of Gas Turbines Power Plant," *Int. J. Comput. Sci. Issues*, vol. Vol. 10, no. Issue 1, Jan. 2013, [Online]. Available: https://citeseerx.ist.psu.edu/document?repid=rep1&type=pdf&doi=765da9c4c0b94025e2db44a0f5d97a8f2f623a0c

[60] L. E. Øi, A. Haukås, S. Aromada, and N. Eldrup, “Automated Cost Optimization of CO_2 Capture Using Aspen HYSYS,” presented at the The First SIMS EUROSIM Conference on Modelling and Simulation, SIMS EUROSIM 2021, and 62nd International Conference of Scandinavian Simulation Society, SIMS 2021, September 21-23, Virtual Conference, Finland, Mar. 2022, pp. 293–300. doi: 10.3384/ecp21185293.

Appendices

Appendix A Task description

Appendix B Detailed installation factor table by Nils Henrik Eldrup

Appendix C Source code of sensitivity analysis with Python

Appendix A: Task description

The general aim is to develop a model in Aspen HYSYS combining a natural gas based power plant and CO_2 capture by amine absorption. A special aim is to use this for energy and cost optimizing of parameters in the process.

1. Literature search on process simulation of natural gas based power plants combined with absorption based CO_2 capture.

2. Aspen HYSYS simulation, dimensioning and cost estimation of different alternatives possibly utilizing the spreadsheet facility in Aspen HYSYS.

3. Process optimization, preferably automated, of process parameters. Typical parameters are temperatures and pressures in the power plant and gas inlet temperature, temperature approach in the main heat exchanger and packing height in the absorption column.

4. Evaluation of limitations for the cost optimization, especially when using the prosess simulation program Aspen HYSYS.

Appendix B: Detailed installation factor table by Nils Henrik Eldrup

Fluid handling equipment Installation factors

Adjustment for materials:

SS316 Welded: Equipment and piping factors multiplies with 1,75

SS316 rotating: Equipment and piping factors multiplies with 1,30

Exotic Welded: Equipment and piping factors multiplies with 2,50

Exotic Rotating: Equipment and piping factors multiplies with 1,75

Porsgrunn September 2020
Nils Henrik Eldrup

Equipment cost (CS) in kEUR from:	0	10	20	40	80	160	320	640	1280	2560	5120
to:	10	20	40	80	160	320	640	1280	2560	5120	10240
Equipment costs	1,00	1,00	1,00	1,00	1,00	1,00	1,00	1,00	1,00	1,00	1,00
Erection cost	0,49	0,33	0,26	0,20	0,16	0,12	0,09	0,07	0,06	0,04	0,03
Piping incl. Erection	2,24	1,54	1,22	0,96	0,76	0,60	0,48	0,38	0,30	0,23	0,19
Electro (equip & erection)	0,76	0,59	0,51	0,44	0,38	0,32	0,28	0,24	0,20	0,18	0,15
Instrument (equip. & erection)	1,50	1,03	0,81	0,64	0,51	0,40	0,32	0,25	0,20	0,16	0,12
Ground work	0,27	0,21	0,18	0,15	0,13	0,11	0,09	0,08	0,07	0,06	0,05
Steel & concrete	0,85	0,66	0,55	0,47	0,40	0,34	0,29	0,24	0,20	0,17	0,15
Insulation	0,28	0,18	0,14	0,11	0,08	0,06	0,05	0,04	0,03	0,02	0,02
Direct costs	7,38	5,54	4,67	3,97	3,41	2,96	2,59	2,30	2,06	1,86	1,71
	-	-	-	-	-	-	-	-	-	-	-
Engineering process	0,44	0,27	0,22	0,18	0,15	0,12	0,10	0,09	0,07	0,06	0,05
Engineering mechanical	0,32	0,16	0,11	0,08	0,06	0,05	0,03	0,03	0,02	0,02	0,01
Engineering piping	0,67	0,46	0,37	0,29	0,23	0,18	0,14	0,11	0,09	0,07	0,06
Engineering el.	0,33	0,20	0,15	0,12	0,10	0,08	0,07	0,06	0,05	0,04	0,04
Engineering instr.	0,59	0,36	0,27	0,20	0,16	0,12	0,10	0,08	0,06	0,05	0,04
Engineering ground	0,10	0,05	0,04	0,03	0,02	0,02	0,01	0,01	0,01	0,01	0,01
Engineering steel & concrete	0,19	0,12	0,09	0,08	0,06	0,05	0,04	0,04	0,03	0,03	0,02
Engineering insulation	0,07	0,04	0,03	0,02	0,01	0,01	0,01	0,01	0,00	0,00	0,00
Engineering	2,70	1,66	1,27	0,99	0,79	0,64	0,51	0,42	0,34	0,28	0,23
	-	-	-	-	-	-	-	-	-	-	-
Procurement	1,15	0,38	0,48	0,48	0,24	0,12	0,06	0,03	0,01	0,01	0,00
Project control	0,14	0,08	0,06	0,05	0,04	0,03	0,03	0,02	0,02	0,01	0,01
Site management	0,37	0,28	0,23	0,20	0,17	0,15	0,13	0,11	0,10	0,09	0,09
Project management	0,45	0,30	0,26	0,22	0,18	0,15	0,13	0,11	0,10	0,09	0,08
Administration	2,10	1,04	1,03	0,94	0,63	0,45	0,34	0,27	0,23	0,20	0,18
	-	-	-	-	-	-	-	-	-	-	-
Commissioning	0,31	0,19	0,14	0,11	0,08	0,06	0,05	0,04	0,03	0,02	0,02
	-	-	-	-	-	-	-	-	-	-	-
Identified costs	12,48	8,43	7,11	6,02	4,91	4,10	3,49	3,02	2,66	2,37	2,13
	-	-	-	-	-	-	-	-	-	-	-
Contingency	2,50	1,69	1,42	1,20	0,98	0,82	0,70	0,60	0,53	0,47	0,43
	-	-	-	-	-	-	-	-	-	-	-
Installation factor 2020	14,98	10,12	8,54	7,22	5,89	4,92	4,19	3,63	3,19	2,84	2,56

Appendix C : Source code of sensitivity analysis with Python

```
import win32com.client
import time
import numpy as np
import matplotlib.pyplot as plt
from datetime import datetime
starting_point=79
end_point=20
num_p=59
temp=np.linspace(float(starting_point),float(end_point),num_p+1)
NPV=np.zeros(num_p+1)

def connect_to_hysys():
    try:
        hysys_app = win32com.client.Dispatch("HYSYS.Application")
        return hysys_app
    except Exception as e:
        print(f"Error: {e}")
        return None
def load_simulation(hysys_app, file_path):
    try:
        simulation = hysys_app.SimulationCases.Open(file_path)
        return simulation
    except Exception as e:
        print(f"Error loading simulation: {e}")
        return None
```

```
def access_adj(simulation, adj_name, Isignored_value):

    # Access the heat exchanger object by name
    adj_active_check = simulation.Flowsheet.Operations.Item(adj_name)
    adj_active_check.IsIgnored= Isignored_value

def matched_adj(simulation, adj_name):
    # Access the heat exchanger object by name
    adj_active_check = simulation.Flowsheet.Operations.Item(adj_name)
    matched_or_not= adj_active_check.IsValid
    return matched_or_not
def matched_target_adj(simulation, adj_name):
    # Access the heat exchanger object by name
    adj_active_check = simulation.Flowsheet.Operations.Item(adj_name)
    matched_target= adj_active_check.IterationTargetValueValue
    tole=adj_active_check.ToleranceValue
    target_val=adj_active_check.TargetValueValue
    #target=float(target_val)
    if len(matched_target)==1:
       last_res=float(matched_target[0])
    else:
       last_res=float(matched_target[-1])
#    if abs(last_res-target_val)<=tole:
#       res=True
    return abs(last_res - target_val) <= tole
def matched_target_adj2(simulation, adj_name):
```

```
        # Access the heat exchanger object by name
        adj_active_check = simulation.Flowsheet.Operations.Item(adj_name)
        matched_target= adj_active_check.IterationTargetValueValue
        tole=adj_active_check.ToleranceValue
        target_val=adj_active_check.TargetValueValue
        #target=float(target_val)
        if len(matched_target)==1:
            last_res=float(matched_target[0])
        else:
            last_res=float(matched_target[-1])
#       if abs(last_res-target_val)<=tole:
#           res=True
        return print((last_res - target_val),tole)
def set_adj_target(simulation, adj_name,target_value):

        # Access the heat exchanger object by name
        adj_active_check = simulation.Flowsheet.Operations.Item(adj_name)
        adj_active_check.TargetValue=target_value

def access_heat_exchanger_duty(simulation, heat_exchanger_name):
    try:
        # Access the heat exchanger object by name
        heat_exchanger = simulation.Flowsheet.Operations.Item(heat_exchanger_name)
        duty = heat_exchanger.Duty
        print(f"Heat Exchanger Duty: {duty} Watts")
    except Exception as e:
       print(f"Error printing adjusted variables: {e}")
```

```
def report_time():
    current_time = datetime.now().strftime("%H:%M:%S")
    return current_time

def reverse_array(array):
    return np.flip(array)

temp=reverse_array(temp)
def main():
        hysys_app = connect_to_hysys()
        if hysys_app is not None:
            try:
                # Specify the path to your HYSYS simulation file
                simulation_file_path = r"D:\USN\Model.hsc"
                spreadsheet_name = "main"
                adj_name = "ADJ-6"
                #Isignored_value=True
                #cell_address_to_change = "A2"
                cell_address_npv="R29"
                #----
                target_value=10

                # Load the HYSYS simulation
                print('Step 0')
                simulation = load_simulation(hysys_app, simulation_file_path)
                time.sleep(20)
```

```
print('Step 1')
spreadsheet = simulation.Flowsheet.Operations.Item(spreadsheet_name)
print('Step 2')
time.sleep(10)
print('Step 3')
print('The simulation has started at: ', report_time())
for i in range (num_p+1):
    target_value=temp[i]
    set_adj_target(simulation, adj_name,target_value)
    time.sleep(10)
    y=1
    while y==1:
      Cond_1= matched_target_adj(simulation,"ADJ-1")
      Cond_2= matched_target_adj(simulation,"ADJ-2")
      Cond_3= matched_target_adj(simulation,"ADJ-3")
      Cond_4= matched_target_adj(simulation,"ADJ-4")
      Cond_5= matched_target_adj(simulation,"ADJ-5")
      #Cond_6= matched_target_adj(simulation,"ADJ-6")
      if Cond_1 and Cond_2 and Cond_3 and Cond_4 and Cond_5:
         y=0
         time.sleep(10)
      else:
         y=1
         print(Cond_1,Cond_2,Cond_3,Cond_4,Cond_5)
         matched_target_adj2(simulation, "ADJ-1")
         time.sleep(15)
```

```
            NPV[i]=spreadsheet.Cell(cell_address_npv).CellValue
            print('--------------------------------------------------------------------------')
            print('Time: ', report_time())
            print('At ',round(temp[i],2),' C minimum approach the NPV is:',round(NPV[i],3),
' %')
        simulation.Save()
        plt.plot(temp,NPV)
        plt.xlabel('Minimum Temperature Approach (deg-C)')
        plt.ylabel('Net Present Value (1000EUR)')# Y label for Pci
        #plt.ylabel('Pci In Front Of The Chock Valve Unit:Pascal')# Y label for volumetric
flow rate
        plt.show()
        # change_hysys_cell_value(spreadsheet_name, cell_address_to_change,
new_cell_value)
      except Exception as e:
        print(f"Error: {e}")
      finally:
        # Disconnect from HYSYS
        #hysys_app.Quit()
        print("Disconnected from Aspen HYSYS.")
  if __name__ == "__main__":
 main()
```